XVII. PLASMAS AND CONTROLLED NUCLEAR FUSION

A. ACTIVE PLASMA SYSTEMS[*]

Academic and Research Staff

Prof. A. Bers   Prof. G. D. Bernard   Prof. J. G. Siambis
Prof. W. D. Getty   Prof. G. Bolz   Dr. J. Taillet

Graduate Students

R. R. Bartsch   M. A. Lieberman   H. M. Schneider
S. R. G. Brueck   R. R. Parker   R. E. Tremain
J. A. Davis   D. M. Perozek   M. G. Smith
B. R. Kusse   R. D. Reilly   R. N. Wallace

RESEARCH OBJECTIVES

Our research on active plasma systems falls under two main headings: Beam-Plasma Systems and Active Solid-State Plasmas. The beam-plasma program is both experimental and theoretical. The experimental part of the program will be oriented toward plasma heating. The theoretical effort will continue to focus on stability theory. Other theoretical work now being done will be closely tied to the experiments. The solid-state plasma program will be theoretical. The active solid-state plasma work has evolved from our work on plasma instability theory and has been stimulated by the speculation that active devices could be developed to exploit these instabilities.

1. Beam-Plasma Systems

Beam-Plasma Discharge Studies. A major part of our effort will continue to be on the study of the Beam-Plasma Discharge (BPD). Part of our work with the BPD will be done in experiments in which it is used as a plasma source and further ion heating is attempted by applying RF power at an ion-resonance frequency (ω_{pi} or ω_{ci}) to the plasma. In other projects we shall study various aspects of the BPD itself:

(a) BPD properties with pulsed gas feed. The working gas is fed into the vacuum system by a pulsed gas valve instead of by a continuously flowing needle valve. The decay of the hot-electron plasma after the heating pulse is under study both experimentally and theoretically.

(b) Computer charge-sheet model. A one-dimensional charge-sheet model of the beam-plasma discharge is under study. The effect of magnetic-mirror reflecting boundaries is to be taken into account. This work is aimed at understanding the nonlinear aspects of the BPD. In particular, the source mechanism for the high-energy electrons and the randomization of collective oscillations are two topics of interest in this work.

(c) BPD properties. Work will continue on various aspects of the BPD such as the "spiking" characteristic of the microwave radiation from the plasma and the rotating instability frequently observed in one of the BPD experiments.

Ion Heating Studies. The beam-plasma discharge produces a plasma with hot electrons and cold ions. Several schemes for heating the ions will be studied. In two of the experiments the beam-plasma discharge is used as a working plasma, and in the third, an electron-cyclotron resonance discharge.

(a) Beam modulation at ω_{ci}. The electron beam is modulated at the ion cyclotron frequency. The modulation frequency will be too high for the neutralizing ions to follow the beam electron density variations and a net space charge will be created. An AC radial electric field inside the BPD may result and this field would drive the ions at cyclotron resonance.

(b) Concentric-electrode excitation of ion cyclotron waves. This experiment is currently under way in System C. The goal is to excite an ion wave in the BPD which will be absorbed by cyclotron or collisional damping.

(c) Beam-plasma interaction at ω_{pi}. An electron beam will interact with the plasma ions if the electron temperature and beam density are high enough. In this experiment a low-density, hot-electron plasma generated at electron-cyclotron resonance, and a low-voltage beam that can be modulated at ω_{pi} are used. A nonconvective or absolute instability may be possible under certain conditions.

Cross-Field Beam-Plasma Interaction. Experimental work on cross-field beam-plasma interactions will continue. An electron beam with considerable velocity transverse to the magnetic field is produced, and will be passed through a plasma. Several potential controlled fusion devices are now in existence which have electron or ion beams injected across the applied magnetic field into a plasma. The beam-plasma behavior of such systems will be studied in this experiment.

Theory of Plasma Instabilities. Theoretical work on the stability theory of systems of finite extent will continue. Computer programs for stability analysis of transcendental dispersion relations are now being developed. Direct display of both complex ω (frequency) and k (wave number) planes, as well as the branch points that give the absolute instabilities are being planned.

The energy viewpoint of microinstabilities in plasmas (velocity-space instabilities) will be further developed. The extension of this viewpoint to drift and universal instabilities will also be studied. We should soon have a fairly complete picture of the instabilities in fast waves across the magnetic field, and of relativistic instabilities in general.

The theoretical study of beam-plasma interactions will continue in two major directions: hot-plasma effects in finite geometry systems, and computer modeling for understanding some of the nonlinear aspects of beam-plasma interactions.

Dynamics of the Plasma Boundary. A computer analysis of the perturbed motion of electrons at the boundary between a plasma and vacuum has revealed that a hydrodynamic description would not be adequate. We find that the perturbation of the boundary tends to introduce a strong random oscillation of the entire plasma. Thus far, only a uniform and cold plasma has been considered in the absence of an applied magnetic field.

We propose to continue the computer study of the perturbation of a plasma-vacuum boundary. The effects of density gradients, applied magnetic fields, and thermal motion will be considered. The aim is eventually to arrive at a suitable theoretical model that may be checked experimentally.

2. Active Solid-State Plasmas

We propose to continue our theoretical study of plasma instabilities in solids. Three active interactions of current experimental interest will be explored: (i) active surface wave interactions in a magnetic field; (ii) high-frequency electron-phonon instabilities in magnetic fields; and (iii) drifted helicon instabilities for degenerate semiconductors, and in finite geometry samples.

A. Bers, W. D. Getty

1. BEAM-PLASMA DISCHARGE: EXCITATION OF IONS AT THE ION CYCLOTRON FREQUENCY (THEORY)

The beam-plasma discharge (BPD) is a process in which a highly ionized, dense plasma is produced. The primary energy source is the DC drift energy of the injected electron beam; part of this energy is fed into the plasma by the strong coherent oscillations that are induced in the electrons.[1,2] In recent experiments electron densities of 10^{13}/cm^3 have been obtained. Electron "temperatures" of hundreds or thousands of electron volts are observed; but ion energies are typically very low, probably less than 10 ev. For some time, we have been searching for a mechanism that will allow us to feed additional energy directly to the ions. Such a selective heating process suggests the use of a resonance: either ion plasma (ω_{pi}) or ion cyclotron (ω_{bi}) resonance. Briggs[3,4] and Bers[3] have shown that in a hot-electron plasma, a collective interaction between the ions and an electron beam can be excited near ω_{pi}. Under any realistic set of circumstances, however, this is a very weak interaction and is probably not very useful. Cyclotron resonance, if it can be excited, is a very strong absorber of power. The question is, then, "How can we modify a BPD, so as to heat ions by the excitation of oscillations of ω_{bi}?"

Since the basic mechanism of energy transfer in the BPD is the coupling between waves traveling in the beam and in the plasma, the initial search for suitable ion interactions was also in terms of wave interactions. Although such interactions can be found, they are characterized by long wavelengths because of the low frequencies involved (1-10 Mc/sec). When waves of very low phase velocity (v/c~10^{-2}) are found, so that λ is less than the apparatus length, the susceptibility to damping is very great.

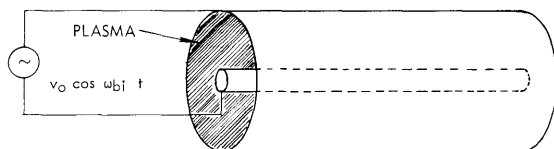In this report, we shall discuss a different approach in which one can make the quasi-static approximation ($\lambda \rightarrow \infty$). If the center conductor in Fig. XVII-1 is driven by an AC voltage $V_o \cos \omega_{bi} t$, the radial electric fields will penetrate the plasma to the extent that sheaths will permit. Because of the axial magnetic field, sheaths will not form to shield the interior of the plasma, and particles will be subjected to a radial electric field. Clearly, if $\omega \rightarrow \omega_{bi}$, there will be a strong interaction with the ions. The charge per unit length of a 10-kv, 10-amp electron beam is

Fig. XVII-1. Concentric electrode system with plasma between the electrodes.

$$q = \frac{I}{v} = 1.5 \times 10^{-7} \frac{\text{coulomb}}{\text{meter}}.$$

By Gauss' law (at a radius of 1 cm),

$$E = \frac{q}{\epsilon_o 2\pi b} \approx 2.7 \times 10^5 \text{ v/m}$$

if the beam is unneutralized, and if $\epsilon = \epsilon_o$.

In the BPD, the beam is fired into the neutral gas and a plasma is gradually built up. Presumably, the plasma electron and ion densities adjust themselves so as to neutralize the over-all beam-plasma system. What would happen if the beam current were suddenly reduced to a fraction $a < 1$ of its initial value?
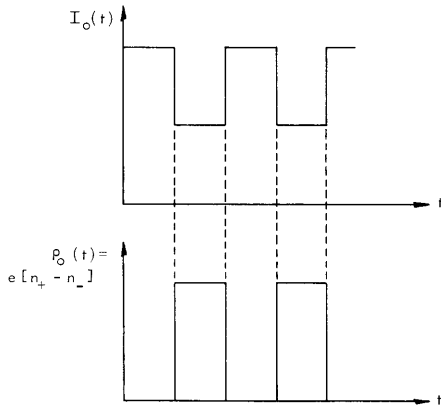
The initial situation within the beam was $n_{-p} + n_{-b} - n_{+p} = 0$. The reduction in beam current leaves the beam region positively charged. Because of the magnetic field $\overline{B}_o$, there can be no radial flow of charges to re-establish neutrality. There is no source of electrons at the ends of the mirror to feed in extra electrons, so ions must be expelled. For $B_o = 3000$ gauss and a plasma potential of +1 kv, an axial motion of ions toward the ends of only 2×10^{-2} cm is found in a half-cycle at ω_{bi}. Thus the ions cannot move any appreciable fraction of the plasma length (~1 meter) and the beam remains unneutralized.

Fig. XVII-2. Time variation of the beam current $I_o(t)$ and the net space charge $\rho_o(t)$.

If the beam current is suddenly increased, plasma electrons will be driven out along the axis. Thus the charge-balance situation will be as shown in Fig. XVII-2.

From this type of reasoning, it seems that by current-modulating the beam of a BPD, we can produce an AC radial field in the discharge and thus excite the ions at ω_{bi}. The electric field will be the sum of an AC and a DC field $\underset{\sim}{E}(t) = E_o(1 + \cos \omega t)$.

L. D. Smullin

[Professor Smullin is on leave of absence at the Indian Institute of Technology, Kanpur, India, during the academic year 1965-1966.]

References

1. W. D. Getty and L. D. Smullin, "Beam-Plasma Discharge: Buildup of Oscillations," J. Appl. Phys. **34**, 3421-3429 (1963).

2. L. D. Smullin and W. D. Getty, "Characteristics of the Beam-Plasma Discharge," Paper CN-21/122, International Atomic Energy Agency Conference on Plasma Physics and Controlled Nuclear Fusion Research, Culham, England, September 6-10, 1965.

3. R. J. Briggs and A. Bers, "Electron Beam Interactions with Ions in a Warm Plasma," Proc. Fourth Symposium on Engineering Aspects of MHD, University of California, Berkeley, California, April 10-11, 1963, pp. 23-30.

4. R. J. Briggs, Electron-Stream Interaction with Plasmas, Monograph No. 29 (The M. I. T. Press, Cambridge, Mass. , 1964), Chap. 5.

2. BEAM-PLASMA DISCHARGE: EXCITATION OF IONS AT THE ION CYCLOTRON FREQUENCY (EXPERIMENT)

In Section XVII-A. 1 a method of exciting plasma ions at the ion cyclotron frequency was proposed. This method is being experimentally studied in System A, which is shown schematically in Fig. XVII-3. A transformer is used to insert an AC voltage in series with the beam-pulse voltage. A "Class C" amplifier (500 watts output) is keyed to supply an RF pulse of variable starting time and duration. Peak-to-peak swings of 4000 volts
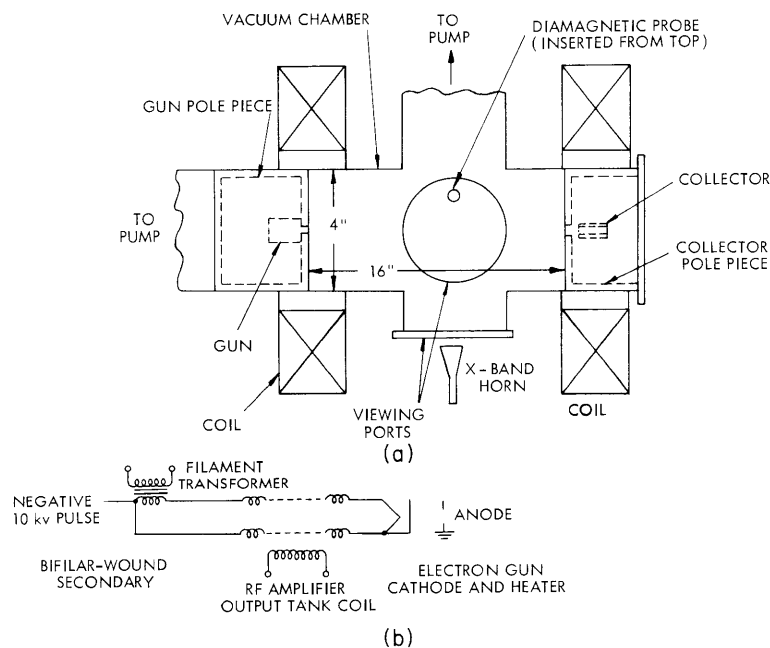
Fig. XVII-3. (a) Schematic diagram of System A.
(b) Electrical circuit used for modulating the beam voltage.

can be superimposed on a 10-kv beam pulse, thereby resulting in a beam-current RF modulation of 0. 5 amp on a normal pulse current of 1 amp at 10 kv. The frequency of the modulation is ordinarily fixed in the range 750-900 kcps, and the axial magnetic field is varied to search for resonance effects. Under ordinary operation (no
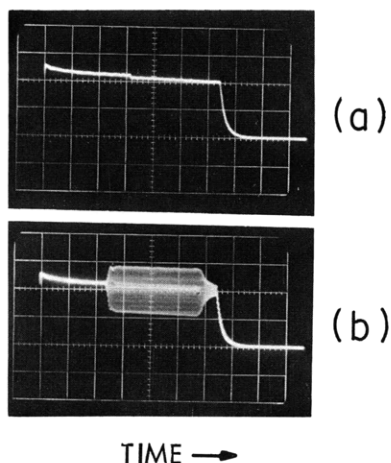
TIME ⟶

Fig. XVII-4.

Beam collector current with and without
RF modulation. Current scale, 0.1 amp/
cm; time scale, 50 μsec/cm; modulation
frequency, 740 kcps; midplane magnetic
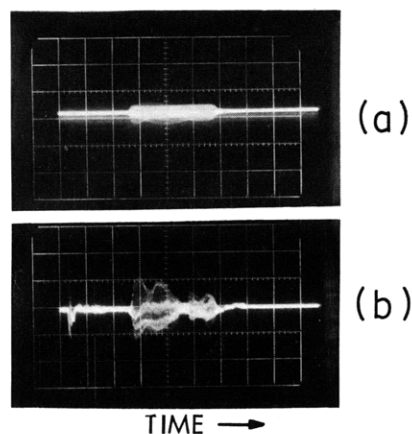field, 385 gauss. (a) I_c no RF. (b) I_c
with RF.

TIME ⟶

Fig. XVII-5.

(a) H_z diamagnetic signal with no working
gas in the system (no PBD).
(b) H_z diamagnetic signal with gas on and
BPD present. Time scale, 50 μsec/
cm. The RF beam modulation is on
for 150 μsec in both cases.

RF modulation), a BPD is obtained in hydrogen gas at pressures of 10^{-4}-10^{-3} torr and
at midplane magnetic fields of 100-700 gauss. Iron pole pieces are used to obtain mag-
netic mirrors with a mirror ratio of 3.[1]

Our principal diagnostic tools in these preliminary experiments have been a diamag-
netic loop that can be oriented to detect H_θ or H_z, an X-band horn with video crystal out-
put for detecting radiation above 6 Gc/sec, a photomultiplier for detecting total light,
and oscillograms of beam-voltage and beam-collector current. An RF modulation pulse
is usually applied 100-200 μsec after the beam pulse begins, and is left on for a few
hundred microseconds. The beam-pulse length is in the range 200-600 μsec, and the
pulse repetition rate is 60/sec.

When no working gas is admitted to the system there is no BPD, and we observe the
vacuum beam with superimposed modulation (Fig XVII-4). The RF H_θ field is measured
with the diamagnetic loop and the value expected from the known RF beam current is
obtained ($I_{rf}/2\pi r$). A small pickup is observed when the loop is oriented to detect H_z,
as shown in Fig. XVII-5a. This pickup is apparently due to electrostatic coupling. When
gas is admitted to establish a BPD, we observe a large increase in the H_z signal, as
shown in Fig. XVII-5b, and very little increase in the H_θ component. Therefore, in the
presence of a BPD and RF beam modulation, we observe a predominantly H_z RF field,
as expected for a diamagnetic signal. The diamagnetic signals in Fig. XVII-5a and -5b
are not integrated, and hence it is not known whether there is any "average" diamagnetic

flux increase during the RF pulse. These effects are observed in the range of B_o such that $\omega \gtrsim \omega_{bi}$ (at the midplane), as well as at other values of B_o.

Changes in the light output are also observed when the beam modulation is applied. These changes are dependent on B_o.

The preliminary experiments have shown that we can easily modulate the electron beam with a percentage modulation approaching 50 per cent. They have shown that strong effects are produced in the plasma by this modulation. Detailed measurements must be made of the diamagnetism and of ion linewidths to determine whether ion heating takes place.

W. D. Getty, G. Bernard

References

1. H. Y. Hsieh, "Experimental Study of Beam-Plasma Discharge," Ph. D. Thesis, Department of Electrical Engineering, M. I. T. , September 1964.

3. BEAM-PLASMA DISCHARGE: SYSTEM C

System Changes

Several changes have been incorporated into System C in connection with the ion-cyclotron experiments.[1] These include (a) insertion of a 12 mm O. D. Pyrex tube into the system for the purpose of making wave-field measurements; (b) relocation of the magnet coils to obtain a uniform field (within 0. 1%) over a distance of 28 cm in the center of the mirror while keeping a mirror ratio of 3; and (c) redesign of the collector-electrode system in order to provide stronger coupling to the plasma. The collector is now a $\frac{3}{8}$ in. × 2 in. copper disk in the center of which a boron-nitride bushing is mounted. The electrode is a $\frac{1}{4}$ in. O. D. solid copper rod mounted in the center of the bushing and extending outside the system through an insulated feed-through. The electrode can thus be inserted a variable distance into the plasma in order to achieve stronger coupling.

Experiments

a. Axial Variation of the Plasma Diamagnetism

Plasma diamagnetism as a function of axial distance has been measured by inserting a 100-turn, 0. 622 cm^2 coil into the Pyrex tube described above. A typical waveform of the integrated coil voltage in shown in Fig. XVII-6. Absolute diamagnetic measurements are complicated by the effect of induced eddy currents in the system wall[2]; however, fast changes (time constants less than 100 μsec) can be easily interpreted. In Fig. XVII-7 we have plotted the initial value of the diamagnetic signal as a function of distance from the collector. Plots of the change in diamagnetism at the end of the beam
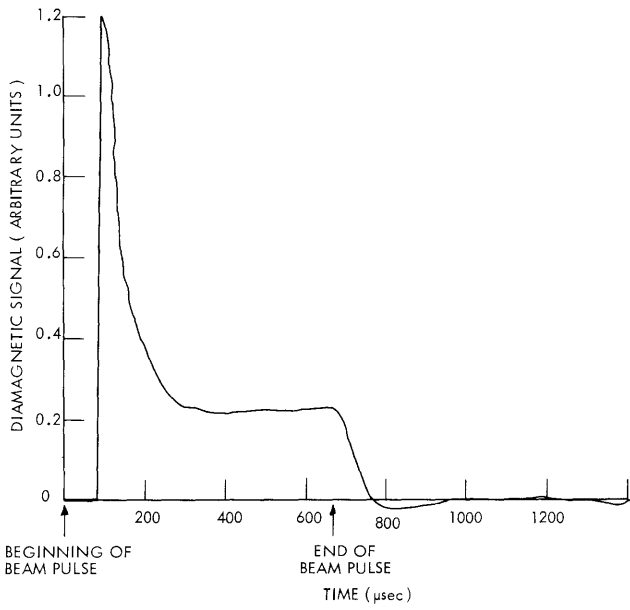
Fig. XVII-6.

Time-dependence of the diamagnetic probe signal.

Fig. XVII-7.

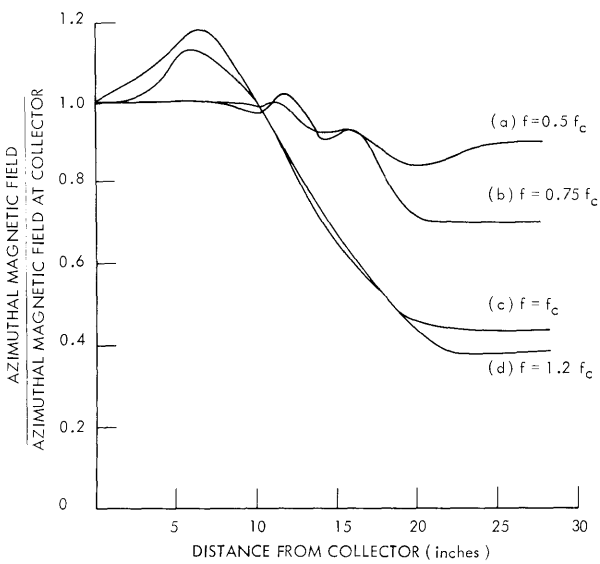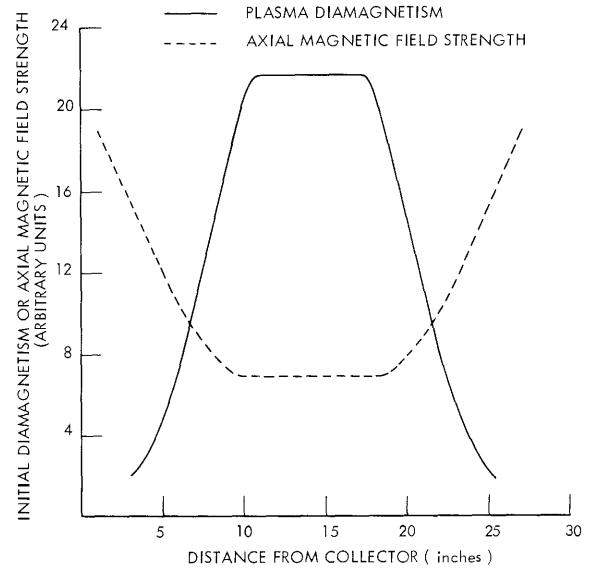Axial dependence of initial diamagnetism and magnetic field strength.

Fig. XVII-8.

Axial dependence of the azimuthal component of the wave magnetic field.

pulse as a function of distance from the collector have also been made, and produce curves very similar to that shown in Fig. XVII-7. For comparison, a plot of the axial magnetic field strength is also shown. The plasma is rather well localized axially within the low-field region of the mirror.

b. Axial Variation of Azimuthal Wave Magnetic Field

Wave-field measurements have been made as a function of axial distance and frequency. The measurements were made with a 5-turn, 2.26 cm^2 coil wound so as to pick up H_θ, the azimuthal component of the wave field. Results are shown in Fig. XVII-8, and the general behavior is as expected. For low frequencies, the plasma supports a TEM-like mode (torsional Alfvén wave) which gives rise to the standing-wave structure observed in Fig. XVII-8a and 8b. At higher frequencies, because of resonance effects from the ions, the wave becomes attenuating, owing to absorption or (for $f > f_c$) evanescence (see Fig. XVII-8c and 8d). The rapid variations observed in the curves in Fig. XVII-8a and 8b are thought to be due to local variations in the magnetic field. As we have mentioned, the field has now been straightened, and these measurements will be repeated.

Phase measurements of the wave field have also been made and from these, the low-frequency wave speed has been deduced. If one assumes this speed to be equal to the Alfvén speed along the magnetic field, one obtains a density of approximately $10^{12}/cm^3$, which is consistent with other measurements.

R. R. Parker

References

1. R. R. Parker, "Beam-Plasma Discharge: System C," Quarterly Progress Report No. 78, Research Laboratory of Electronics, M.I.T., July 15, 1965, pp. 99-100.
2. L. D. Smullin, W. D. Getty, and R. R. Parker, "Beam-Plasma Discharge: System C," Quarterly Progress Report No. 76, Research Laboratory of Electronics, M.I.T., January 15, 1965, pp. 104.

4. BEAM-PLASMA DISCHARGE: SYSTEM D

Operation of System D continues with a pulsed gas source, which is used to obtain a pressure gradient in the vacuum system at the instant of time when the electron beam is fired. Ideally, we would like to admit gas molecules in a jet along the axis of the system and then fire the electron beam through the jet before the gas has had time to spread throughout the vacuum system. With this scheme, we hope to reduce the amount of neutral gas around the plasma and in the electron gun.

In a previous report,[1] we gave the reason for establishing a pressure gradient by
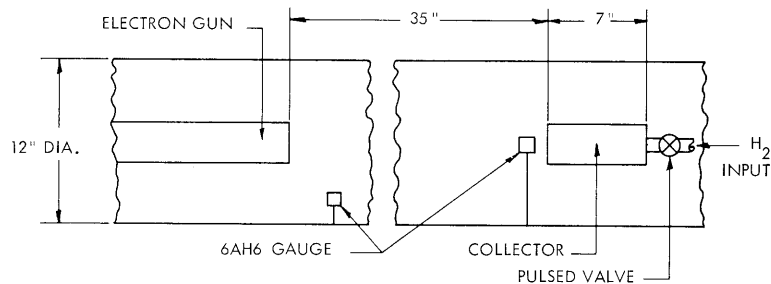
Fig. XVII-9.   Schematic diagram of System D showing the location of the two
6AH6 nude pressure gauges.

this method. It is done in order to reduce the axial ion current that would ordinarily flow from the plasma into the electron gun. This axial current originates from ionization of hydrogen gas that flows into the plasma column from the region between the plasma boundary and the metal walls. The plasma column acts like a pump, with an estimated "pumping speed" of 50,000 liters/sec. By reducing the gas pressure outside the plasma, we have eliminated this undesirable axial current flow.
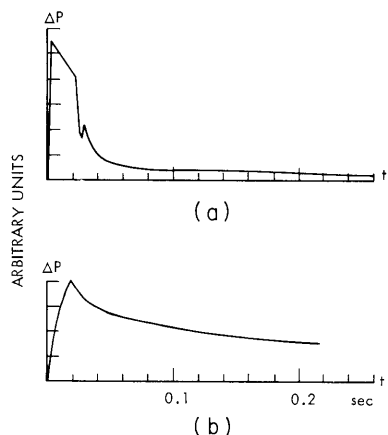

Fig. XVII-10. (a) Asco valve pressure transient.
Gauge located on axis and 1 inch
in front of the collector.
(b) Asco valve pressure transient.
Gauge located 2 inches off axis
and 20 inches in front of the
collector.

We have attempted to determine the spatial distribution of the gas at the time when the beam pulse is fired. The arrangement of gauges is shown in Fig. XVII-9. A nude pressure gauge with a fast response is placed either near the end of the collector or at the outer metal wall of the system near the electron gun. The gauge consists of a 6AH6 vacuum tube with its glass envelope removed.[2] The pulsed valve is an Asco solenoid valve[3] (Catalog No. 8262A2), and is mounted immediately behind the collector. It is driven by a 400-volt, 1-msec pulse. The pressure transients at the two locations are shown in Fig. XVII-10. The gas pressure immediately in front of the collector (Fig. XVII-10) rises in less than 1 msec and is constant for 20-30 msec. At the end of this time, the valve apparently closes and the pressure decays, the time constant being
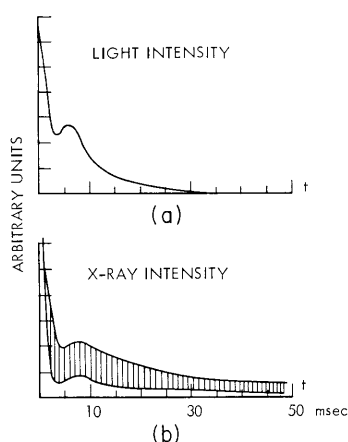
Fig. XVII-11. Light and x-ray intensity vs time with 5-msec delay between the gas pulse and beam firing.

determined by the system pumping speed and volume. A second, smaller pulse appears later, because of the bounce of the valve plunger. At the location near the electron gun the pressure (Fig. XVII-10b) rises exponentially until the valve closes, at which time the pressure decays with the same time constant as that observed at the collector location. The time scale of these transients is long compared with the transit time of hydrogen molecules through the system. The thermal velocity of H_2 at room temperature is $\approx 130/cm/msec$, and the system is 18 cm in diameter and 100 cm from collector to electron gun. Most of our experiments are done with a 10-20 msec time delay between the opening of the valve and firing of the electron beam. Thus it seems that considerable spreading of the gas could take place before the beam is fired. The pressure transient also shows that a large amount of gas enters the system after the beam is fired. The effect of a further increase in gas pressure after the plasma has been formed is shown by the small peaks at 10 msec in the light and x-ray decay shown in Fig. XVII-11.

On the time scale of the pressure pulse, there is time for penetration of gas into all parts of the vacuum system; this suggests that it should not make any difference if the gas is admitted by a pulsed valve located at the side of the system, instead of with one located behind the beam collector. A test of this hypothesis was partly negative; but there was evidence that the collector gas feed is better. We observed that with a side gas feed the resulting plasma had qualitatively the same properties as those observed with a collector gas feed. Long decays of light, x-rays, and diamagnetic flux were observed; these signals were appreciably smaller than with a gas feed through the collector. Hence, we c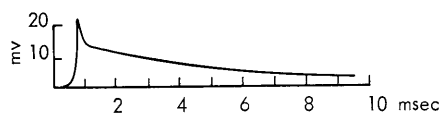onclude that a collector gas feed results in a hotter and/or denser plasma; more measurements of the gas distribution must be made to settle this question. Meanwhile, the collector gas feed is used, since it produces a more interesting plasma.

Fig. XVII-12.
Integrated diamagnetic signal. The calibration of the loop is ev/cm^3 per mv. The loop is 10 inches in diameter and encircles the plasma column.

Work continues on a fast pulsed valve that will admit 10^{17}-10^{18} molecules in less than 1 msec, and completely shut

off thereafter. A modified Asco valve has been used to obtain opening times of less than 1 msec, but with poor reproducibility of the amount of admitted gas. Using this valve, we found that a hot-electron, diamagnetic plasma was formed with a beam-pulse delay of 600-1000 μsec, which is approximately the time of flight of gas molecules from the gas valve to the electron gun. Operation with this valve was relatively free of gun anode-cathode sparking (sparking is observed when the gas pressure in the gun is too high) and axial ion currents. This is encouraging for future work with a fast pulsed valve. It indicates that it may be possible to fully ionize a dense cloud of gas before the gas reaches the electron gun; this would allow us to increase the number of gas molecules and therefore the plasma density without troublesome sparking in the gun and without the axial ion current from plasma pumping.

Figure XVII-12 shows a typical diamagnetic flux signal under conditions when a long plasma decay is observed. The maximum energy density is in the range 10^{14} ev/cm^3. Preliminary x-ray absorption measurements indicate that the average x-ray energy is 17 kev in the afterglow.

W. D. Getty, R. R. Bartsch

References

1. L. D. Smullin, W. D. Getty, T. Musha, and R. R. Bartsch, "Beam-Plasma Discharge: System D," Quarterly Progress Report No. 78, Research Laboratory of Electronics, M.I.T., July 15, 1965, pp. 102-105.

2. J. Marshall, in Plasma Acceleration, edited by S. W. Kash (Stanford University Press, Stanford, California, 1960).

3. Automatic Switch Company, Florham Park, New Jersey.

5. ENERGY GAIN BY MIRROR COLLISIONS IN THE PRESENCE OF A LONGITUDINAL TRAVELING WAVE

Consider a uniform, longitudinal wave with an electric field given by

$$\vec{E} = E_O \cos (\omega t - kz) \vec{i}_z. \tag{1}$$

Let a low-energy electron ($|v| \ll \omega/k$) move parallel to this field and be contained within two fixed walls (idealized magnetic mirrors). The electron can gain much more energy from the wave if the walls are present than if they are not. This is seen qualitatively with reference to a simple physical model. An electron moving slowly relative to the wave's phase velocity experiences a force varying sinusoidally in time until it collides with a wall. It is alternately accelerated and decelerated, and has an energy of $\frac{m}{2}\left(v_1 + \frac{eE_O}{\omega m}\cos \omega t\right)^2$, where v_1 is its net drift velocity. If E_O and v_1 are small, the

kinetic energy is small. Suppose, however, that the electron suffers a perfectly elastic collision with a wall just as the electric field is changing from accelerating to decelerating. The electron will continue to be accelerated. This process can be repeated many times. Of course, the electron can also lose energy by this method, and a random walk will actually occur.

We shall assume that the phase of each wall collision is random with respect to the wave. Strictly speaking, the problem is deterministic, and the phases are not random. In a real system, the mirrors are many wavelengths apart, and a slowly moving electron can see thousands of oscillation periods between wall collisions. If the phase of one wall collision is 0, the phase of the second may be, for example, 6892.73 radians, and the third 13,482.21. Since only the difference between the phase and the highest multiple of 2π is important, it is plausible that this small difference can be treated as a random variable. Also, any slight random variation in the electron or phase velocity should, in effect, completely randomize the phase of the collisions.

Velocity Gain

Consider a coordinate system moving with the wave, in which we can define a potential (Fig. XVII-13). As our reference point we shall consider the minimum of the
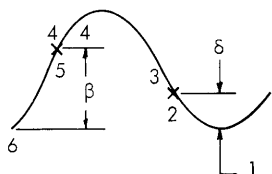

Fig. XVII-13. Potential energy for electrons. (x's are collision points. δ and β are the potentials above the potential minimum at which each collision occurs.)

potential energy for electrons (the negative of the electric potential). After an even number of collisions, we can again look at the energy of the electron at this point to see if it has gained or lost peak energy.

We shall denote velocities relative to the moving system by primes; those relative to the fixed system will not have primes.

Consider an electron with velocity v_1 in the fixed frame, at position 1 in Fig. XVII-13. In the moving frame its velocity is $v'_1 = v_1 - v_o$, where $v_o = \omega/k$. Its velocity at point 2, just before a collision at a potential δ is

$$v'_2 = -\sqrt{v'^2_1 - \frac{2\delta}{m}}.$$ (2)

(The velocity in the moving (primed) system is always negative for electrons moving slower than the wave's phase velocity.) In the fixed system its velocity is

$$v_2 = v'_2 + v_o.$$ (3)

After the collision,

$$v'_3 = -v'_2 - v_o \tag{4}$$

and

$$v'_3 = -v'_2 - 2v_o. \tag{5}$$

At point 4, just before another collision at potential β,

$$v'_4 = -\sqrt{v'^2_3 - \frac{2(\beta-\delta)}{m}} . \tag{6}$$

After this collision,

$$v'_5 = -v'_4 - 2v_o. \tag{7}$$

At point 6, on returning to the bottom of the potential well,

$$v'_6 = -\sqrt{v'^2_5 + \frac{2\beta}{m}} . \tag{8}$$

In the fixed system,

$$v_6 = v'_o + v_o. \tag{9}$$

In order to solve Eqs. 2-9, we must make some approximations. We shall assume that v^2_1, $\delta^2/m^2v^2_o$, $\beta^2/m^2v^2_o$, $\beta v_1/mv_o$, and $\delta v_1/mv_o$ can all be neglected compared with v^2_o. This assumes that the initial velocity of the electron is small compared with the phase velocity of the wave, and that the potential energy of the wave is small compared with the kinetic energy of an electron moving at the wave's phase velocity. The last assumption means that a stationary electron in the fixed system is not trapped by the wave.[4] With these assumptions, the final velocity of the electron is

$$v_6 \approx v_1 + 2\frac{(\delta-\beta)v_o}{mv^2_o}. \tag{10}$$

Here, v_6 is the velocity of an electron after suffering two abrupt, perfectly elastic collisions. The first collision occurs at a potential energy δ above the potential minimum, the second at a potential energy β above the minimum. v_1 and v_6 are both measured at the potential energy minimum. δ and β will be treated as random variables.

Probability Theory

Let us normalize the random variables by setting

$$\delta = \frac{aV_1}{2} + \frac{V_1}{2} \tag{11}$$

$$\beta = \gamma \frac{V_1}{2} + \frac{V_1}{2}, \tag{12}$$

where V_1 is the peak-to-peak potential energy, and a and γ are random variables such that $-1 \le a \le 1$; $-1 \le \gamma \le 1$. From Eqs. 10-12,

$$v_6 \approx v_1 + \frac{V_1}{mv_o^2}(a-\gamma)\, v_o. \tag{13}$$

We assume that a collision at any argument of the wave is equally probable. We find that the probability density function of a is

$$f_a(a_o) = \frac{1}{\pi\sqrt{1 - a_o^2}}. \tag{14}$$

The probability that a will have a value within the interval da_o at a_o is $fa(a_o)\, da_o$ (a and γ have the same probability distribution). The characteristic function of a is

$$M_a(v) = J_o(v). \tag{15}$$

Let

$$R = \sum_{i=1}^{N/2} a_i - \sum_{j=1}^{N/2} \gamma_j,$$

where a_i is the value of a at the ith collision, and N is the total number of collisions with both walls. The characteristic function of R is

$$M_R(v) = \left[J_o(v)\right]^N. \tag{16}$$

The variance of R is

$$E(R^2) = N/2. \tag{17}$$

The expected value of $\overline{v_6^2}$, after N collisions, is

$$\overline{v_6^2} = \overline{v_1^2} + \frac{V_1^2}{\left(mv_o^2\right)^2}\, v_o^2 \frac{N}{2}. \tag{18}$$

Let us ignore $\overline{v_1^2}$ to the second term on the right-hand side of Eq. 28. Then a large number of particles, all of which have had the same number of wall collisions, will have

an average velocity given by Eq. 18. Let us replace the potential energy V_1 by aeV_o, where a is a dimensionless constant between 0 and 1, and $eV_o = mv_o^2/2$. In one dimension, we can define a temperature by

$$\frac{eT}{2} = \frac{m\overline{v^2}}{2} \tag{19}$$

or

$$T = \frac{a^2 N V_o}{4}, \tag{20}$$

where N is the total number of collisions, $V_o = \dfrac{m(\omega/k)^2}{2e}$, and a is the peak-to-peak electrostatic wave potential divided by V_o.

We can do a similar analysis of a model that has the electrons re-entering the wave, after a collision with a wall, at a phase independent of the one it had just before the wall collision. In this case,

$$T = \frac{a^2 N V_o}{8}. \tag{21}$$

Discussion

A mechanism such as has been described may furnish the reason that beam-plasma interactions in mirror machines produce much hotter electrons than if the mirrors were absent.[2] Other explanations such as a Doppler-shifted cyclotron resonance effect, proposed by Stix[3] and criticized by Smullin,[4] are also possible. Also, in a gradual mirror, the wave may extend up into the mirror, and may grow or decay in space and time. These effects are not included in our model. Computer "experiments" for investigating these effects are in progress.

J. A. Davis

References

1. Trapping appears very rapidly in the charge-sheet calculations presented in Sec. XVII-A. 6. This assumption is therefore probably not a good approximation.

2. W. D. Getty and L. D. Smullin, "Beam-Plasma Discharge: Buildup of Oscillations," J. Appl. Phys. 34, pp. 3421-3429 (1963).

3. T. H. Stix, "Energetic Electrons from a Beam-Plasma Overstability," Phys. Fluids 7, 1960 (1964).

4. L. D. Smullin, "A Criticism of 'Energetic Electrons from a Beam-Plasma Overstability'," Phys. Fluids 8, 1412 (1965).

6. DISCRETE PARTICLE MODELS OF THE BEAM-PLASMA DISCHARGE

The purpose of this research is to obtain a better understanding of the mechanism that heats the plasma electrons in a beam-plasma discharge. In particular, one of the heating schemes to be tested is the wave-mirror interaction described in Sec. XVII-A. 5. We hope to construct charge-sheet computer models that can predict the electron temperatures and beam-velocity spread that is present in System A.

Description of the Model

The model considered here has initially a cold plasma. The beam is injected with 1 per cent velocity modulation at the plasma frequency. The beam is collected after passing through the plasma, but the plasma electrons are reflected at the collector and at the gun. This is an idealization of magnetic mirrors. The problem is one-dimensional, with electrons represented by infinite "sheets," in the manner of Buneman,[1] Dawson,[2] Dunn,[3] and others.

The beam has a charge density equal to 1/200 that of the plasma, and is represented by 1 beam sheet for each 10 plasma sheets. The ions are represented as a continuous, neutralizing, stationary background. The electric field at the gun is constrained to be zero. This is felt to be reasonable, since the plasma has no net charge, and the magnetic mirror "walls" can hold no charge.

If all sheets had the same charge, the acceleration would be

$$a = - \frac{e\rho_o}{m\epsilon_o} \left[z - n\Delta z + \frac{\Delta z}{2} \right],$$ (1)

where ρ_o is the ion charge density; Δz, the average sheet separation; n, the number of sheets between the gun and the considered sheet (including that sheet); e, the electron charge; m, the electron mass; and ϵ_o, the dielectric constant of free space. The position and velocity are given by

$$z(t+\Delta t) = z(t) + v(t) \Delta t + \frac{a(\Delta t)^2}{2}$$ (2)

$$v(t+\Delta t) = v(t) + a\Delta t,$$ (3)

where Δt is the incrementation time. We normalize distances to the Debye length, $\lambda_D = V_T/\omega_p$, of electrons with average thermal velocities equal to 0. 1 of the injected beam DC velocity. There are 5 plasma sheets for this Debye length, but the field seen by each sheet is the average taken over 3 Debye lengths. This averaging is done to reduce the "noise" resulting from use of discrete sheets. Time is normalized to the incrementation time. There are 1000 plasma sheets, and initially 100 beam sheets. With
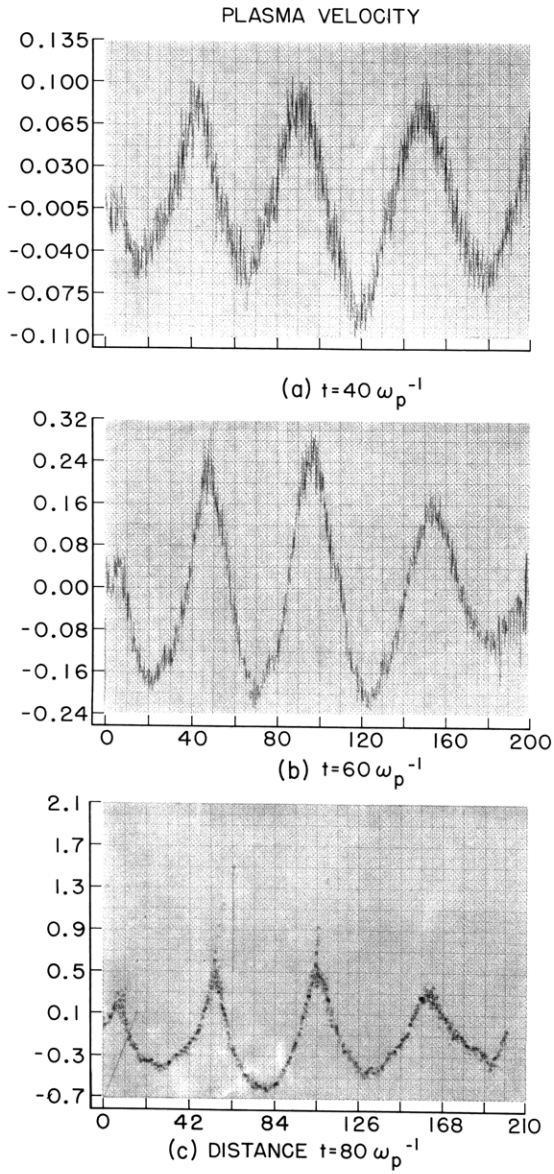
PLASMA VELOCITY

(a) $t = 40\,\omega_p^{-1}$

(b) $t = 60\,\omega_p^{-1}$

(c) DISTANCE $t = 80\,\omega_p^{-1}$

BEAM VELOCITY

(a) $t = 40\,\omega_p^{-1}$

(b) $t = 60\,\omega_p^{-1}$

(c) DISTANCE $t = 80\,\omega_p^{-1}$

ACCELERATION

(a) $t = 40\,\omega_p^{-1}$

(b) $t = 60\,\omega_p^{-1}$

(c) DISTANCE $t = 80\,\omega_p^{-1}$

Fig. XVII-14. Instantaneous plasma-sheet velocity vs distance.
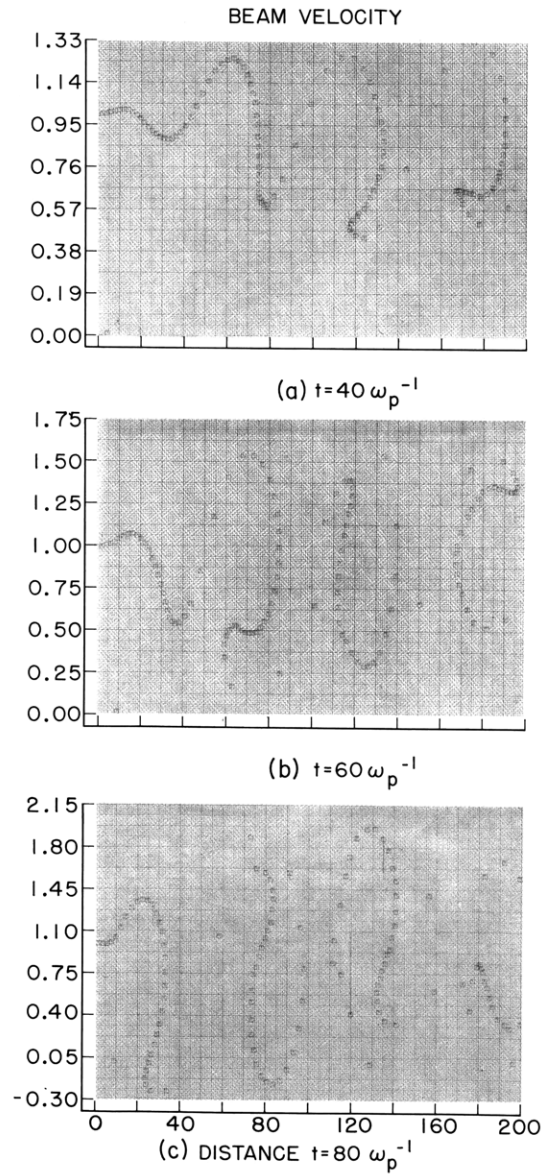
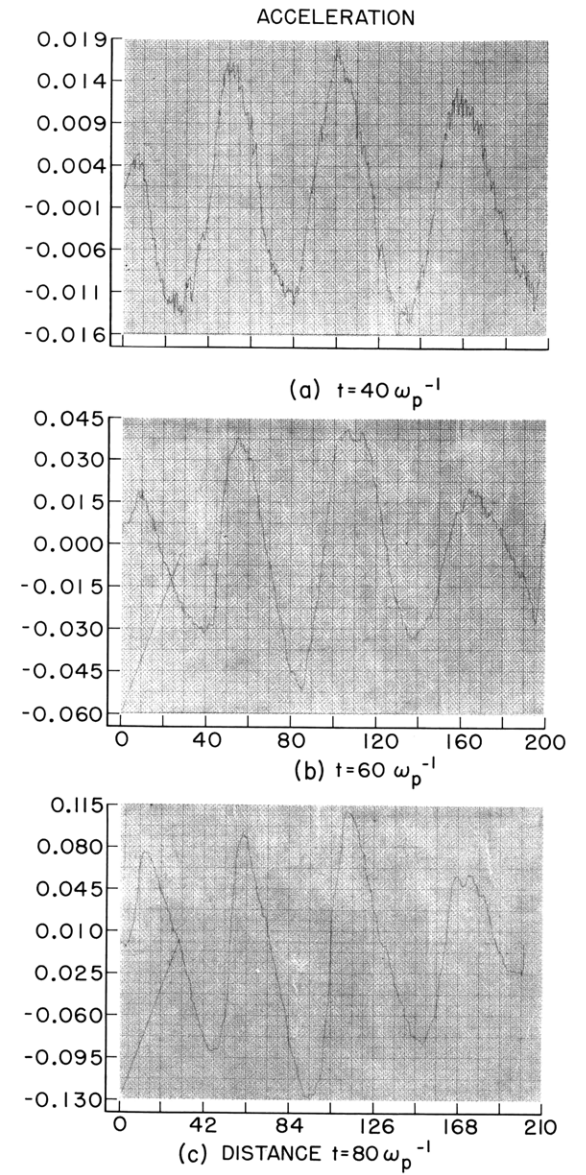Fig. XVII-15. Instantaneous beam-sheet velocity vs distance.

Fig. XVII-16. Instantaneous acceleration vs distance.

$$z = X\lambda_D \tag{4}$$

and

$$v = V\frac{\lambda_D}{\Delta t}, \tag{5}$$

Eqs. 1-3 reduce to

$$A(t) = -(\omega_p\Delta t)^2\left[\ddot{X}(t) - n\Delta\overline{X} + \frac{\Delta X}{2}\right] = a\frac{(\Delta t)^2}{\lambda_D} \tag{6}$$

$$X(t+\Delta t) = \overline{X}(t) + V(t) + A\frac{(t)}{2} \tag{7}$$

$$V(t+\Delta t) = V(t) + A(t). \tag{8}$$

The inclusion of beam sheets in (6) is straightforward, as is the averaging of A over 15 sheets.

Preliminary Results

For the first runs, $(\omega_p\Delta t)$ was chosen to be 0.2. Figures XVII-14 through 16 show the instantaneous plasma-sheet velocity, beam-sheet velocity, and acceleration vs distance, at t = 40 ω_p^{-1}, 60 ω_p^{-1}, and 80 ω_p^{-1}. The velocities are normalized with respect to the injected beam velocity. Note that after 400 incrementation times $(80\,\omega_p^{-1})$ (Figs. XVII-14c, XVII-15c, and XVII-16c), the space-charge waves have built up enough to trap the plasma sheets (Fig. XVII-14c). By this we mean that the plasma sheets have been accelerated to the wave phase velocity, and are trapped in the potential wells of the wave. Before this happens, the beam sheets have overtaken one another, forming bunches that are also trapped by the space-charge wave (Fig. XVII-15a). When the bunches first form they occur near the point of maximum deceleration, thereby giving up a maximum of energy to the wave. Later (Fig. XVII-15a and 15b), the bunches oscillate about the point of zero acceleration.

Later times are not shown; apparently the integration techniques have failed and energy is not conserved. Smaller values of $(\omega_p\Delta t)$ are now being tried, and perhaps more sophisticated integration techniques will have to be used.

J. A. Davis

References

1. O. Buneman, "Dissipation of Currents in Ionized Media," Phys. Rev. 115, 503 (1959).

2. J. Dawson, "One-Dimensional Plasma Model," Phys. Fluids 5, 445 (1962).

3. D. A. Dunn and I. T. Ho, "Computer Model of a Beam Generated Plasma," Internal Memorandum, Stanford Electronics Laboratory, Stanford University, 1963.

7. DYNAMICS OF THE PLASMA BOUNDARY

The study of the plasma boundary with a discrete charge-sheet model[1] continues.

Again, the electrons are uniformly displaced from the ion background in a neutralized plasma slab. The motion of the electrons which results from this initial perturbation is desired. Others have also recently pointed out[2] that such motion is inherently nonlinear and can only be adequately described by large-scale numerical computations.

In Fig. XVII-17 we show the results for the motion of the electrons when a plasma slab is modeled by 41 electron and ion sheets, and a uniform initial displacement is made so that two electron sheets are outside the original slab boundary. (The ions are assumed to be of infinite mass and hence the ion sheets remain stationary; their positions are not shown in any of the figures.) Note that the surface scrambling gradually spreads into the center of the slab, so that eventually the coherent oscillations of the electron sheets at the plasma frequency are destroyed. If the initial perturbation is larger than a two-sheet displacement, the scrambling occurs at a more rapid rate. This is illustrated in Fig. XVII-18 which shows the electron sheet positions as a function of time when a slab is modeled by 41 sheets, but the initial displacement consists of 5 sheets outside the neutralizing ion background.

The effect of placing an insulating wall near the plasma slab has been considered. This is accomplished in the discrete model by constraining all electron sheets that make excursions outside the original slab greater in magnitude than the initial perturbation to "stick" to the walls. The sheets that are caught in this manner still influence the motion of the other sheets through their space-charge forces. In Fig. XVII-19 we give the results for walls placed near the slab described by the motion shown in Fig. XVII-18. It appears that the presence of the walls allows the coherent motion of the sheets to persist for a longer time. This is reasonable, since the sheets that are removed are the ones that create the scrambling through their crossing trajectories, and when caught act only to provide a restoring force for other sheets executing motions outside the original slab boundary.

H. M. Schneider

References

1. H. M. Schneider and A. Bers, "Dynamics of the Plasma Boundary," Quarterly Progress Report No. 78, Research Laboratory of Electronics, M. I. T., July 15, 1965, pp. 114-119.

2. W. M. Leavens and I. Leavens (Private communication, 1965).

8. HOT-ELECTRON PLASMA DECAY IN A MAGNETIC-MIRROR MACHINE

Coulomb collision scattering losses for a hot-electron plasma in a magnetic-mirror machine have been investigated by using a multistep approximation to the electron
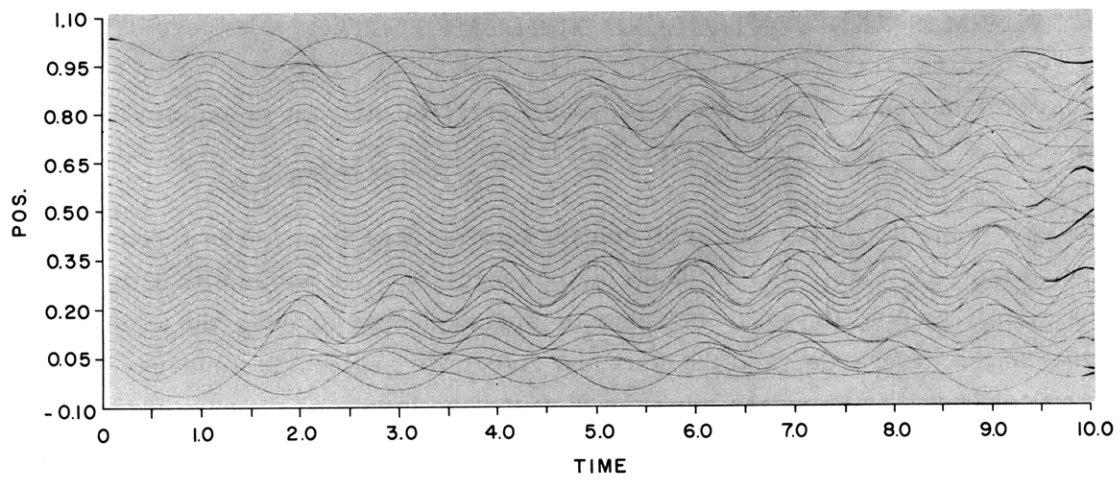
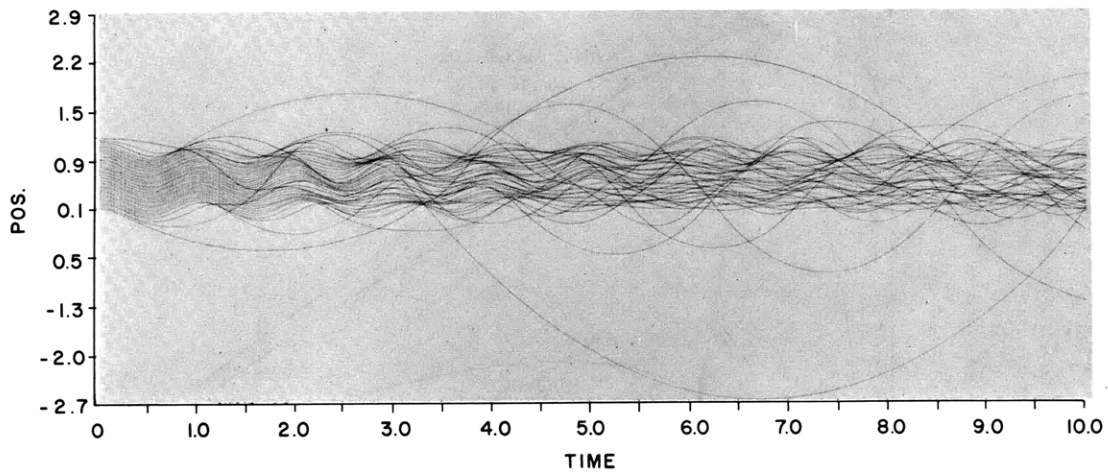Fig. XVII-17. Slab dynamics: two-sheet displacement.

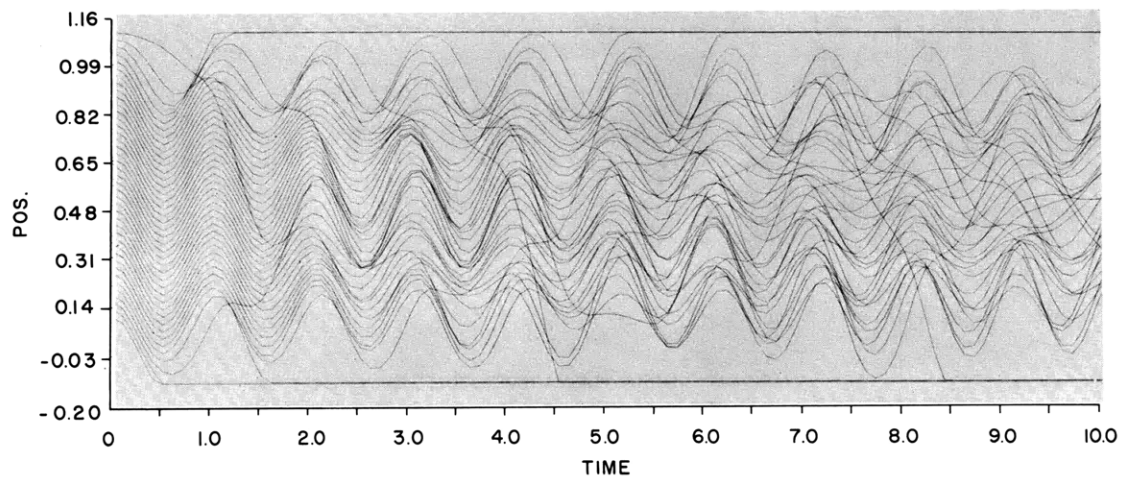Fig. XVII-18. Slab dynamics: five-sheet displacement.

Fig. XVII-19. Slab dynamics: effect of insulating walls on initial five-sheet displacement.

distribution function. This process is, at present, of interest to explain the observed lengthening of the plasma decay in System D (see Sec. XVII-A. 4) when a pulsed gas feed is used.[1]

We have considered the Coulomb scattering resulting from three types of collisions: electron-electron, electron-ion, and electron-neutral. We assume that the system is approximately neutral ($n_e = n_i$), because of space-charge forces, the electrons have energies in the kev range, and the ions are cold. We neglect the tendency of electron-electron collisions to Maxwellianize the distribution function, slowing of the electrons by inelastic collisions, and the production of a low-energy electron plasma by
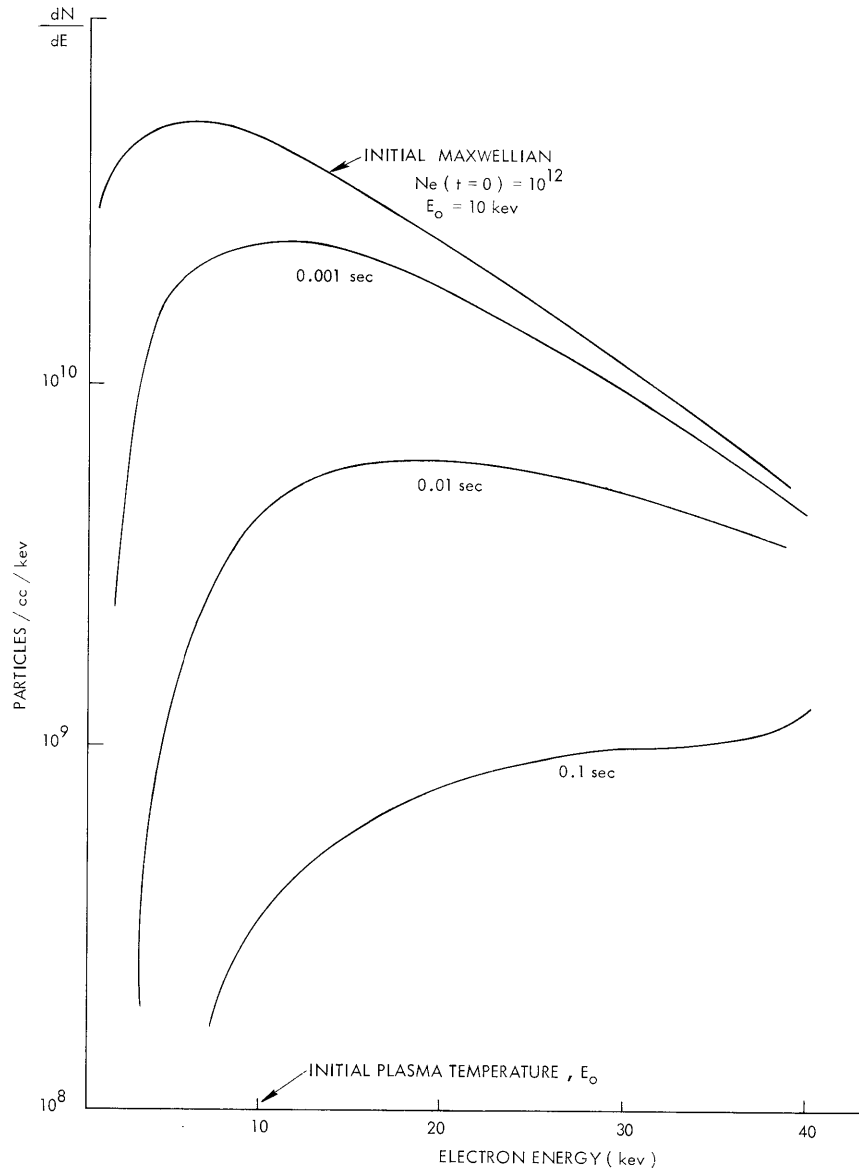

Fig. XVII-20. Distribution function during decay.

electron-neutral ionizing collisions. Electrons that have been scattered through a net rms angle of 1 radian are assumed to have left the mirror system through the loss cones. Each step of the distribution function is allowed to decay independently for a given increment of time at a rate determined by the number of electrons/cm^3 in each of the other energy steps, the ion density (equal to the total electron density), and the neutral density.

The angular scattering rates are determined in the same manner as Fessenden used for calculating mirror scattering losses by electron-neutral collisions.[2] We assume small-angle collisions, and use the appropriate shielding cutoff distance for the Coulomb potential. This distance is the electron Debye length for electron-electron and

$E_o = 1$ kev
N_e (t = 0) = 10^{12} / cc
MIRROR RATIO ~ 10

$N_o = 0$

$N_o = 10^{10}$/ cc

$N_o = 10^{11}$ / cc

$N_o = 10^{12}$ / cc
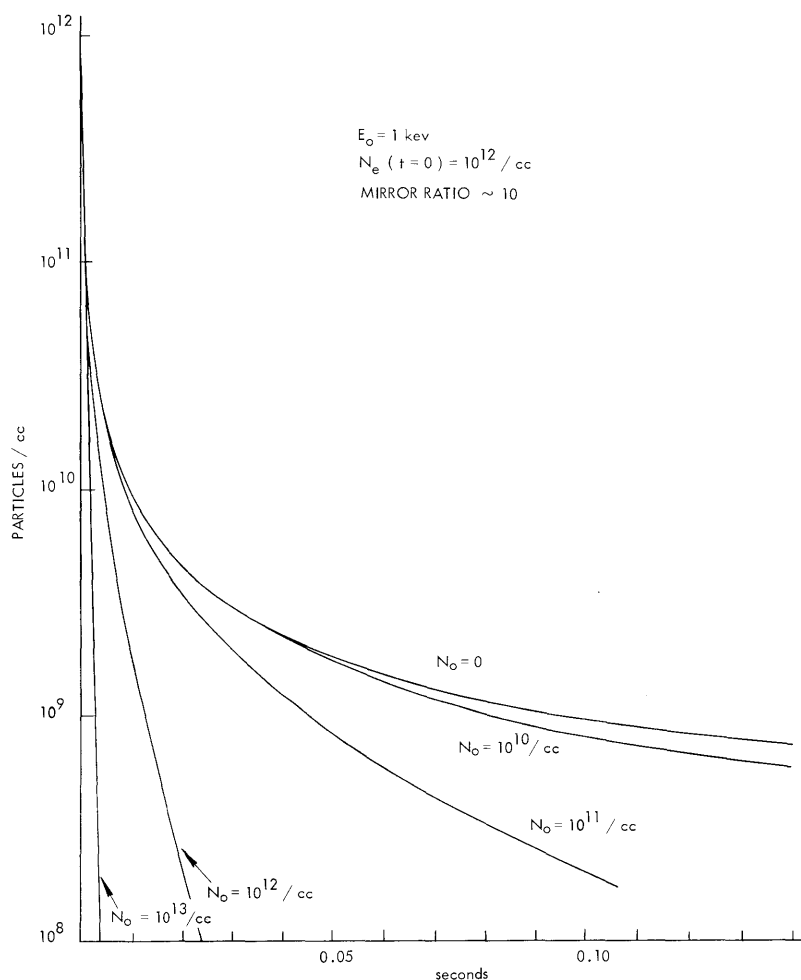
$N_o = 10^{13}$/cc

Fig. XVII-21. Effect of neutral background density decay.

electron-ion collisions, and the atomic radius for electron-neutral collisions. The angular scattering rates for each type of collisions for electrons with energies in jth step of

the distribution function are given in Eqs. 1-3 for a 40-step model:

Electron-ion:
$$\nu_s(E_j) = \frac{50N_{ion}}{(E_j)^{3/2}} \tag{1}$$

Electron-neutral:
$$\nu_s(E_j) = \frac{10N_o}{(E_j)^{3/2}}\left(1+\frac{1}{4}\log E_j\right) \tag{2}$$

Electron-electron:
$$\nu_s(E_j) = \frac{600N_e(E_j)}{E_j(\Delta E)^{1/2}} + \sum_{i<j} \frac{54N_e(E_i)}{|E_i-E_j|(E_j)^{1/2}}$$

$$+ \sum_{i>j}^{40} \frac{54N_e(E_i)}{|E_i-E_j|(E_i)^{1/2}}, \tag{3}$$

where ΔE is the width of the electron distribution function steps in kev, E_j is the energy of the jth step in kev, N_{ion} is the ion density normalized to $10^{10}/cm^3$, N_o is the neutral density normalized to $10^{10}/cm^3$, and $N_e(E_i)$ is the number of electrons per cm^3 in the ith step of energy in units of 10^{10} electrons/cm^3.

Sample decays for an initially Maxwellian, hot-electron plasma are shown in Figs. XVII-20 and XVII-21. Figure XVII-20 shows the distribution function at various times, and Fig. XVII-21 shows the effect of background pressure on the scattering losses. Measurements of the electron density decay in System D will be compared with the predictions of this model.

R. R. Bartsch

References

1. L. D. Smullin, W. D. Getty, T. Musha, R. R. Bartsch, "Beam Plasma Discharge: System D," Quarterly Progress Report No. 78, Research Laboratory of Electronics, M.I.T., July 15, 1965, pp. 102-105.

2. T. J. Fessenden, Sc.D. Thesis, Department of Electrical Engineering, M.I.T., June 1, 1965.

9. FIRST-ORDER CORRECTION TO THE FIRST ADIABATIC INVARIANT

It is a well-known fact that a charged particle gyrating in a static magnetic field, under certain circumstances, undergoes a motion described by one[1] or more[2] (maximum of three) adiabatic invariants.

The first adiabatic invariant M, is given by an asymptotic series

$$M = M_o + \epsilon M_1 + \epsilon^2 M_2 + \epsilon^3 M_3 + \ldots$$

the first term of which, M_o, is identified with the magnetic moment (for the nonrelativistic case)

$$M_o = \frac{1}{2} \frac{v_\perp^2}{B},$$

where B is the magnetic field evaluated at the position of the particle r, and v is the component of the particle's velocity perpendicular to the magnetic field at the position of the particle $\vec{r}$.

The second term in the series, M_1, has been computed in general form by Kruskal.[1] It is given by

$$M_1 = -\frac{1}{B^3}\left\{ v^2 e_1 \cdot [(\vec{v} \times e_1) \cdot \nabla]\vec{B} + (\vec{v}\vec{v}\cdot e_1) \cdot [(\vec{v} \times e_1) \cdot \vec{\nabla}]\vec{B} \right.$$
$$\left. + (\hat{e}_1 \cdot \vec{v})(\vec{\nabla}\times\vec{B}) \cdot \left(\frac{v_\perp^2}{2}\hat{e}_1 + 2\vec{v}\,(\hat{e}_1 \cdot \vec{v}) \right) \right\},$$

where $e_1 = B/B$ and the velocities $\vec{v}$, $\hat{e}_1 \cdot \vec{v} = v$, and $\vec{v}_\perp$ and the magnetic field B are evaluated at the position of the guiding center of the particle $\vec{R}$, or at the actual position of the particle $\vec{r}$, the difference being of second order in the asymptotic series expansion in terms of ϵ and therefore being absorbed into the second-order correction, M_2. The original choice of variables in expressing M_1 is such as to make the actual numerical computation of this term fairly involved. Similarly, the physical mechanisms that give birth to M_1 are greatly obscured by this choice of variables.

We shall give here an alternative, but completely equivalent, expression for M_1, which is obtained when one uses a coordinate system natural to the field lines of the magnetic field.[3] This coordinate system is defined as follows:
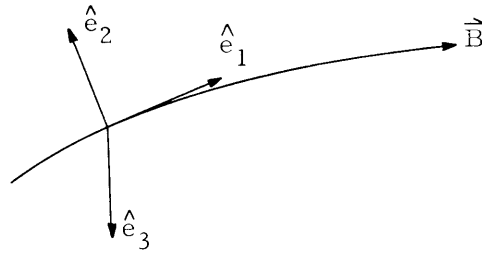
$$\hat{e}_1 = \frac{\overline{B}}{B}, \qquad \hat{e}_2 = R(s)\frac{d\hat{e}_1}{ds} = \frac{1}{k(s)}\frac{d\hat{e}_1}{ds}, \qquad \hat{e}_3 = \hat{e}_1 \times \hat{e}_2$$

where $\hat{e}_1$ is the unit tangent, $\hat{e}_2$ the principal normal, $\hat{e}_3$ the principal binormal at a given point on a field line, $R(s)$ is the radius of curvature, $k(s)$ is the curvature, and ds is the element of length along the field line. If one then utilizes this coordinate system and all of its implications, one obtains for M_1

$$M_1 = -\frac{v_\perp^2}{B^2}\left\{ \left(\frac{v_{||}^2 + v^2}{v_\perp}\right) k(s) \sin\phi + v_{||} \sin^2\phi\, \sigma_3(s) \right.$$

$$+ v_{||} \cos^2\phi\, \sigma_2(s)$$

$$+ v_{||} \sin\phi \cos\phi\, [k_2(s) - k_3(s)]$$

$$\left. +\left[\frac{3v_{||}}{2}\hat{e}_1 - \vec{v}_\perp\right]\cdot\left(\frac{\nabla\times B}{B}\right)\right\},$$

where

$$\phi = -\theta_0 - \int_0^{\cdot t} (\omega - v_{||}\tau(s))\, dt;$$

$k_2(s)$, $k_3(s)$ are the curvatures of the coordinate lines defined by the unit vectors $\hat{e}_2$ and $\hat{e}_3$, respectively; $\sigma_2(s)$, $\sigma_3(s)$ are the shears in the field lines as observed by "looking" along $\hat{e}_2$ and $\hat{e}_3$, respectively; $\tau(s)$ is the torsion along e_1; ω is the angular frequency of rotation of the particle; and $v_{||} = \vec{v}\cdot\hat{e}_1$. And finally all of these quantities are evaluated at the position of the guiding center of the particle $\vec{R}$, or the actual position of the particle $\vec{r}$, the difference being of second order in the asymptotic series expansion in terms of ϵ and therefore being absorbed into the second-order correction M_2.

When M_0 itself is also evaluated at the position of the guiding center $\vec{R} = \vec{r} - \vec{\rho}$, where $\rho = e_1(R)\times v_\perp(R)/\omega$, one obtains for M_1 the following expression:

$$M_1 = -\frac{v_\perp^2}{B^2}\left\{ \frac{2v^2}{v_\perp} K \sin\phi + v_{||}(\sigma_2 + \sigma_3)\right.$$

$$+ v_{||}[\sin^2\phi\, \sigma_2 + \cos^2\phi\, \sigma_3]$$

$$-\frac{1}{2}v_{||}\sin 2\phi\, [K_2 - K_3]$$

$$\left. +\frac{3}{2} v_{||} \frac{e_1\cdot(\nabla\times B)}{B}\right\}.$$

Work continues also on the first-order correction J_1 to the longitudinal invariant J_0.

J. G. Siambis

References

1. M. Kruskal, "The Gyration of a Charged Particle," Project Matterhorn Report PM-S-33, Princeton University, March 1958.

2. T. G. Northrop, The Adiabatic Motion of Charge Particles (Interscience Publishers, Inc., New York, 1963).

3. J. G. Siambis, "The First-order Correction to the First Adiabatic Invariant," (Abstract to appear in Bull. Am. Phys. Soc.).

10. INSTABILITIES IN AN ELECTRON BEAM WITH TRANSVERSE ENERGY

Bers and Gruber[1] have calculated the dispersion relation for nonrelativistic electrostatic plasma waves (E along k) at an angle to B_0, assuming a velocity distribution function

$$f_0(v) = \delta(v_\perp - v_{0\perp})\, \delta(v_\parallel - v_{0\parallel})/2\pi v_0.$$

The dispersion equation is

$$K_\ell(\omega, k) = 1 - \frac{\omega_p^2}{k^2} \sum_{-\infty}^{\infty} \left[\frac{k_\parallel^2 J_n^2\left(\frac{k_\perp v_{0\perp}}{\omega_c}\right)}{(\omega' - n\omega_c)^2} + \frac{k_\perp^2 \left\{ J_{n-1}^2\left(\frac{k_\perp v_{0\perp}}{\omega_c}\right) - J_{n+1}^2\left(\frac{k_\perp v_{0\perp}}{\omega_c}\right) \right\}}{2\omega_c(\omega' - n\omega_c)} \right] = 0$$

with $\omega' = \omega - k_\parallel v_{0\parallel}$. Absolute instabilities are expected for certain values of the parameters $\frac{k_\perp v_{0\perp}}{\omega_c}$, $\frac{\omega_p}{\omega_c}$, and $\frac{k_\parallel}{k_\perp}$. This dispersion relation containing $v_{0\parallel}$ can be applied to an electron beam confined by a magnetic field parallel to the beam. Therefore instabilities can be expected if the beam electrons have enough transverse energy and if the plasma frequency is high enough. To find the lowest plasma frequency at which instabilities can occur, the dispersion equation can be plotted for different values of the parameters.
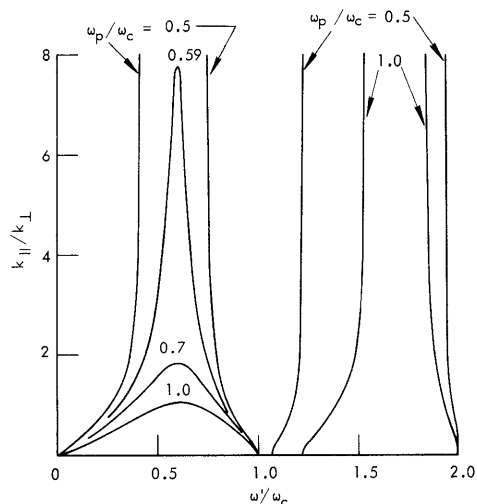
Figure XVII-22 shows the dispersion relation for different values of the parameter ω_p/ω_c, and Fig. XVII-23 for different values of $k_\perp v_{0\perp}/\omega_c$. The curves show maxima approximately at $\omega'/\omega_c = 0.6$. Instabilities are to be expected at values of $k_\parallel/k_\perp$ higher than the maxima because in this case ω' must be complex (from

Fig. XVII-22. Dispersion relation for $k_\perp v_{0\perp}/\omega_c = 1.0$ and different values for ω_p/ω_c.

Fig. XVII-22, for instance, if $\omega_p/\omega_c = 0.7$, $k_{||}/k_\perp > 1.8$). At $\omega_p/\omega_c = 0.5$, no finite maximum appears, therefore no instability can be expected. The lowest plasma frequency at which an instability may appear is approximately $\omega_p = 0.59 \, \omega_c$.
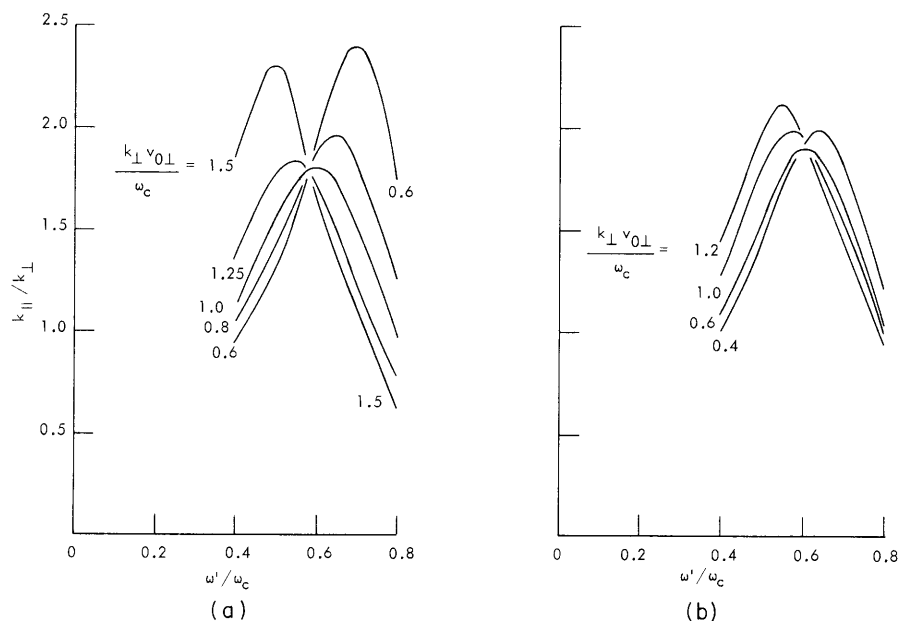

Fig. XVII-23. Dispersion relation for $\omega_p/\omega_c = 0.7$ and different values for $k_\perp v_{0\perp}/\omega_c$. (a) Monoenergetic distribution. (b) Maxwellian distribution in v .

From Fig. XVII-23a the lowest value of the maximum in $k_{||}/k_\perp$ is obtained near $k_\perp v_{0\perp}/\omega_c = 1.0$. A similar analysis, but with a transverse Maxwellian velocity distribution,[2,3] shows (Fig. XVII-23b) the lowest maximum at $k_\perp v_T/\omega_c = 0.6$, this value not being critical. The lowest plasma frequency for an instability, in this case, is approximately $\omega_p = 0.62 \, \omega_c$.

G. Bolz

References

1. A. Bers and S. Gruber, Appl. Phys. Letters 6, 27 (1965).

2. E. G. Harris, J. Nucl. Energy, Part C, 2, 138 (1961).

3. S. Gruber, M. W. Klein, and P. L. Auer, Research Report, Sperry-Rand Research Center, January 1965.

XVII. PLASMAS AND CONTROLLED NUCLEAR FUSION

B. Applied Plasma Physics Related to Controlled Nuclear Fusion[*]

Academic and Research Staff

Prof. D. J. Rose   Prof. L. M. Lidsky   Prof. S. Yip
Prof. T. H. Dupree   Prof. E. P. Gyftopoulos   L. M. Lontai
                          Prof. H. Cheng

Graduate Students

W. R. Flynn   L. C. Pittinger   J. C. Woo
R. A. Hill   C. S. Ribbeck   N. D. Woodson
M. Murakami   C. E. Wagner   D. R. Wilkins

RESEARCH OBJECTIVES

1. Plasma Kinetic Theory

This research program is devoted to investigating the various theoretical aspects of the turbulent plasma problem. In particular, we are studying the interaction between particles and waves to map out the region of validity of the Fokker-Planck equation and to derive improved equations. We are also studying the coupling between waves and their relations to the turbulence spectrum in wave-number space. Many of the analytic results will be verified by appropriate computer experiments.

T. H. Dupree

2. Superconducting Magnetic Systems

We intend to continue the new studies, which were started in 1965, on optimum methods of current stabilization (full superconductor utilization at full stabilization, at the cost of low average current density, versus less than full utilization with high current density, superconductor elementary wire size for optimum stabilization, and so forth). This modest program is both theoretical and experimental.

We intend to prepare short lengths of superconducting cable (other multiconductor assemblies), using different plating materials, plating techniques, interconductor bonding techniques, and so on, in order to test our sometimes qualitative and sometimes quantitative predictions about the performance of such composites. Depending on the outcome of such sample experiments, we may reprocess a large stock of niobium-zirconium wire which is now on hand.

D. J. Rose

3. Material and Engineering Experiments Related to Controlled Fusion

An initial set of experiments for measuring the gamma-ray spectrum emitted by the slowing-down of 14-Mev neutrons in a mock-up fusion blanket assembly was completed in 1965. We intend to start a new set of experiments, using lithium-drifted germanium solid-state detectors, to give better energy and spatial resolution. This technique of studying the gammas from inelastic neutron scattering seems, at present, to be a better way of studying the neutron energy spectrum than measuring the activity of threshold detectors.

We also plan to study damage caused by 14-Mev neutrons in prospectively useful materials for a fission vacuum wall.

D. J. Rose

---

4. Minimum B Confinement Systems

We have built a facility to allow us to study the confinement of hot electron plasmas in minimum B and cusped magnetic fields. The plasma will be generated by beam-plasma interaction to enable direct comparison with the results obtained by L. D. Smullin and W. D. Getty in mirror magnetic fields. We are considering the possibility of electron-cyclotron heating in the same device to investigate the effects of the differing velocity distributions on the confinement properties of hot electron plasmas.

L. M. Lidsky, C. Wagner

5. Plasma Turbulence

Experiments to measure the turbulent structure of a long highly ionized plasma column will be continued and extended. Effects of plasma density, magnetic field, and radial electric field have been measured; the effect of the radial electric field in generating unstable wave growth has been observed. To be studied in more detail are the effects of changing plasma radial profile and the presence of various suspected drift wave instabilities. The autocorrelation and crosscorrelation functions of density and electron temperature will be measured under various selected plasma conditions within the electron density regime 10^{12}-10^{14} cm^{-3}, 10-90 per cent ionized, electron temperature 2-20 ev.

D. J. Rose, J. C. Woo

6. Feasibility Studies of Controlled Fusion

Calculations on hypothetical pulsed fusion systems will be extended in an attempt to settle the question of whether any pulsed controlled fusion system has inherent fatal flaws or not. Calculations will have to do with the steady-state thermal gradient in the vacuum wall, thermal excursions during pulses, penetration of the magnetic field into the vacuum wall and into the coolant, and so forth.

Analysis of apparently feasible fusion neutron moderating blankets containing fissile material will continue.

D. J. Rose, L. M. Lidsky, N. D. Woodson

7. Cesium Plasmas and Adsorption Systems

a. Transport Theory for Low-Energy Plasmas

A transport theory for low-energy plasmas has been developed. The theory has been applied to cesium plasmas in thermionic converters with great success. Novel ionization mechanisms and features of the output-current characteristics have been disclosed. We plan to extend the theory to include magnetic field effects and to apply it to MHD plasmas. We also plan to extend the theory to plasmas consisting of more than one gas.

b. Adsorption Systems

We have continued our work on the correlation of physical properties of metallic surfaces coated by gaseous adsorbates. Preliminary results are encouraging. This study will continue during the coming year.

c. Plasma Stability by Means of Liapunov's Second Method

We have used Liapunov's second method in a variety of physical systems described by nonlinear differential equations.

We are trying to extend the method to fusion plasmas. The major objectives are: (i) to present a unified picture of the different types of stability analysis which have appeared in publications; and (ii) to extend these analyses to more complex plasma models, including nonlinear effects.

E. P. Gyftopoulos

1. ENGINEERING PROBLEMS OF CONTROLLED FUSION

Introduction

This report records our attempt to establish the vital importance of engineering studies of controlled fusion. To make our point, discussions are outlined boldly, as Van Gogh painted. But the problem could be put more subtly, in Degas pastelles; and some have put it unrecognizably, as Kandinsky would.

We have reached some conclusions, based admittedly on less than exhaustive studies. Our principal conclusions may thus be stated.

(i) The present state of the plasma art enables the proposal of systems for analysis.

(ii) Typical analyses have been done, which show that the constants of nature do not preclude various energy-recovery schemes, tritium-breeding schemes, and so forth. This is a positive good and a welcome fact. It is very improbable that the systems which have been studied were optimized.

(iii) The same studies show clearly that (a) the engineering will be a vastly more difficult task than is generally recognized; (b) many problems need attention now, not later; and (c) the cost of any eventual system may be uncomfortably high.

(iv) Engineering studies at this simple level are relatively inexpensive, and a moderate continuation of such effort will answer the questions about feasibility of controlled fusion systems. And certainly they need to be done.

(v) A final decision cannot be made yet, on the basis of present information. But we believe that pulsed systems appear to be very unlikely, absolute minimum magnetic field systems may have an incurable ill, and the D-T blanket problem may be so difficult that we must fall back on a D-D system (but we cannot imagine how a D-D system can be made economically).

This discussion is based largely upon previous studies of the fusion blanket problem made in our laboratory.[1-6] Other sources of information were private discussions and papers that are in early stages of preparation.

The plan is this: Let us propose a series of A-B choices, as nearly as we can, about building a fusion reactor, and see where they lead us. It is surprising how much can be reasonably guessed. To be sure, there must be some C choices (unmentioned) that would refer to quite different devices. The "best" choice at each stage does not necessarily yield the best over-all system. But the choices to be made are not unreasonable; besides, all that we claim is to give an example showing that frightful problems exist to be worked on.

In supporting the choices, we shall use numbers taken from the cited technical reports.[1-6] But we shall not describe the 50-group 5-region fusion codes written to discover neutron spectra, x-ray deposition calculations, threshold detector measurements of neutron spectra in a mock-up blanket section or measurements of the x-rays in the

mock-up. Here, we speculate upon the consequences of the results of this thesis research.

The Choices

(i) D-D vs D-T

We choose D-T because we shall show that the best D-T reactor that we can envisage cannot be much cheaper than a reasonably foreseeable breeder reactor (it may also be more expensive). A posteriori, we cannot afford to cut the burning rate by a factor of approximately 100. This simple decision — almost taken for granted these days — creates profound difficulties.

To those who might propose that the solution to the D-T blanket problem is a return to D-D systems, we ask that they discover an economic utilization. We cannot.

(ii) Steady-State vs Pulsed Systems

We choose steady-state, but do not dismiss pulsed systems. We shall discuss them later.

(iii) Energy-Extraction Blankets

This is not an A-B choice; we choose fused salt made of LiF, BeF_2, UF_4 in proportions to be decided on the following bases:

(a) Oxygen and nitrogen wreak havoc with the neutron economy, allowing insufficient tritium regeneration; thus H_2O, nitrate salts, etc., are all dismissed.

(b) Gas cooling is much too inefficient.

(c) Organic coolants will moderate neutrons (and suffer from radiolysis), but will not regenerate tritium.

(d) We cannot pump liquid metals through magnetic fields. We cannot even pump liquid metals along the field if the flow is turbulent enough to give good heat transfer.

Thus we fix our attention on ionically bonded fused salts. All variants, thus far, come out 50-60 cm thick, including a vacuum wall. A tritium-breeding ratio of 1.15-1.25 tritons per incident 14-Mev fusion neutron seems realizable, and this is moderately good news. Note that the excess regeneration will probably be needed because tritium decays at 1 per cent/month, and most of the D-T fusion charge will not be burned, but recirculated through complicated vacuum pumps and gas-handling systems.

Note that the 1.15-1.25 regeneration ratio is under the assumption of blanket in 4π geometry. Evidently, we must chop some holes somewhere to get things in and out. Admittedly, passages can be angled to preserve effective 4π geometry, but this brings about structural complications.

(iv) Superconducting vs Normally Conducting Magnets

Superconducting magnets are essential, on the basis that magnetic field structures will be at least as complicated as those envisaged, at present. The closed average-minimum-field systems and open absolute-minimum-field systems are fair examples.

But these systems have approximately 90 per cent of the field energy outside the plasma volume; $\nabla \times B = 0$ and $\nabla \cdot B = 0$ guarantee this unfortunate situation, and so much magnetic field energy would be very costly with normal magnets.

There is an accompanying difficulty: the coils must be shielded by an additional 50-60 cm (probably Pb, borated H_2O, etc.); thus the total blanket thickness is 1.0-1.2 meters, and not much can be done about it.

(v) Big vs Small

With a blanket, 1 meter thick, the plasma diameter must be very large, in order for the system to be at all economical. Perhaps a 2-3 m vacuum diameter will be needed. Certainly, a 1-m vacuum diameter looks economically unsound.

(vi) Mirror vs Torus

We have calculated both; Rose and Clark[7] show that unless the mirror ratio is high (certainly >5), the fractional burnup is small (a few per cent). We feel that the system becomes undesirable under those circumstances because calculations also show that unless the minimum field is 50-70 kg (with $\beta \approx 0.2$), we get poor power output [power is proportional to (field)^4]. We do not think much of 250-300 kg mirrors all around the system in such large sizes. Strength of materials would seem to preclude them.

There is another more fundamental reason to stay away from absolute minimum $|B|$ systems: of necessity, the lines come out all over the place, and not just through a neat pair of mirror coils. With anything but virtually complete burnup (preposterous), we must scavenge tritium with great efficiency. Thus much of the inner surface must be a pump of some sort. On the other hand, anything but a carefully chosen vacuum wall (perhaps Mo or Nb) seems to ruin the neutron economy for tritium regeneration. Thus the pumping and blanket requirements in an absolute minimum $|B|$ system may be incompatible.

A torus of such large minor diameter will be immense indeed, but it looks like the best hope at this moment. Note that these arguments put a certain urgency upon obtaining stability in the minimum average B systems.

(vii) Fissile vs Nonfissile Blanket[3]

We choose as much U^{238} as possible in the fused-salt coolant, on the basis that the power output can be increased severalfold without any such increase in the cost. Any small blanketed fusion system seems to be more attractive with UF_4 than without it. But we must be careful how the system is built.

Consider, first, the fusion system: a large vacuum cylinder, surrounded by a fused-salt blanket, let us say. Any wall material, or the fused salt, extracts (and tends to deposit locally) approximately 10 per cent of the incident 14-Mev neutron energy per centimeter thickness for small thicknesses. Thus the vacuum wall, with both neutrons and radiation falling upon it, and the coolant just behind it, sustain the heaviest thermal loading. We suspect, and detailed calculations back up our intuition, that we should not

put uranium in these places.

We can, however, put UF_4 in the attenuator region, say, 4-20 cm behind the vacuum interface. Here, the U^{238}(nf) increases the total power, without loading the vacuum wall or its coolant any more. That is, we flatten the power to some extent, and this process of more uniformly loading the system leads to reduced capital cost/kilowatt. Calculations[3] show that the Li^6 must be highly enriched because Li^6 and U^{238} compete in capturing slow neutrons to produce T or Pu, respectively. In fact, the sum (T + Pu)/ (incident 14-Mev neutron) is 1.4-1.5 in our best calculations thus far, for varying compositions of the fused salt. Since (T/neut) must be ≈ 1.2, Pu generation is limited. In such a system, it seems possible to induce a fast fission with every tenth fusion neutron. Thus with ≈ 20 Mev/fusion (including neutron absorption) and 200 Mev/fission, we double the immediate power out by adding UF_4 to the fused salt. This is the most assured gain to be expected from the strategem.

It is tempting to think of burning the Pu also (it turns out that we would double the total power output which would result in a total multiplication of the fusion power by a factor of 4). Perhaps we can burn it in situ, thus easing the neutron economy; this leads us to consider a barely subcritical breeder assembly, driven by a fusion reactor. We must be careful about this: The UF_4 inventory is huge (8-20 mole per cent of the fused salt), and the Pu builds up from U^{238} at an incredibly slow rate (≈ 30 years?). If the system is initially charged, we have the well-known inventory and cost problems of a fission fused-salt breeder, perhaps running at reduced power/unit volume because it is large and subcritical.

(viii) Fusion-Fission Breeder vs Pure Fission Breeder

This is the final choice, and we do not offer an opinion now. But the question must be asked because we see that a subcritical breeder driven by fusion may be the best of all fusion systems. Then we should ask, How much do we pay for absolute safety or a probable easing of the neutron economy?

We pay in magnetic field, plasma generation, probably reduced power-unit volume. We do not count tritium as a valuable product (except for charging more fusion breeders). To be sure, tritium could be used in bombs, but we are planning for a peaceful economy.

Breeders are not yet developed to a point where we can guess their cost with certainty. It is by no means sure that the first serious study, consisting of half a dozen theses, has produced the optimum fusion system.

Note that we have never mentioned specific cost/kw. The choices have been of one system versus another, and this is the more meaningful comparison; we take the cheapest, all things considered, whatever the cost. But it is interesting to know that a very preliminary cost study of a large toroidal D-T system with parameters [T = 20 kev, $\beta = 0.2$, B = 50 kg, burnup/pass = 0.5 (!), 1.7 Mw/m^2 absorbed on vacuum wall, 132 tons fused salt, 1000 Mw thermal, no uranium] came to \$52/kw, for the reactor alone.[2]

Some guesses unsupported by much technological development had to be cranked in to obtain that number. With U^{238} addition, one expects a reduction; and the thermal loading could probably be increased. Thus we see that a cost of $25/kw might be predicted by some (for the reactor), and this is technologically interesting. But more pessimistic views indicate costs up to $200/kw. No one can predict the truth of the matter yet.

(ix) Steady-state vs pulsed Systems

We prefer steady-state because our analysis, thus far, for a pulsed system[6] gives pessimistic results, unless the confinement time is so long that the system has become a steady-state system.

There are some necessary conditions. The principal ones are:

(a) more electric power out than in,

(b) coils do not fail from excess stress (note that the coils must be the vacuum wall),

(c) blanket does not compress so much that the vacuum wall fails,

(d) neutron heating of the wall during the pulse not excessive, and

(e) wall surface heating by radiation not excessive.

Presumably, we expect anomalous plasma diffusion (otherwise we would have a steady-state system).

It can easily be shown that inertial forces will not restrain the system long enough to give any appreciable power out. Thus the stresses must be taken up more or less statically.

Even with wall strain of 0.07 per cent, wall-temperature increment close to 800°C during the pulse, an anomalous diffusion coefficient 0.005 kT_e/eB (exceedingly weak turbulence) and B = 8 webers/m^2, the ratio (electric energy out)/(magnetic energy in) was only 3, with a confinement time of 0.07 sec in a 2-m radius system. At 2 cents per joule, capacitor cost came to $48/kw. No allowances were made for pumping or blanket cost, and so forth. The wall loading in this case was immense (≈ 40 Mw/m^2 neutron flux incident on the vacuum wall on the average, and much higher during peaks). The molybdenum wall is almost at the limit of flash evaporation.

These results on a pulsed system are at odds with calculations recently reported by F. L. Ribe,[8] who chooses a much smaller system, more highly stressed.

Final Discussion

We conclude that much can be said about the fusion reactor, but more needs to be done. The main conclusions were stated at the beginning. But we see urgent need for study along the following lines.

(i) The critical materials problem with the vacuum wall (10^{22}-10^{23} NVT/cm^2 of 14-Mev neutrons during operating lifetime?).

(ii) More and better neutron cross sections for selected nuclei in the entire range

to 14 Mev. Note that our conclusions depend upon these cross sections; for example, a substantial increase in the (n, 2n) cross sections or decrease in neutron capture will free up the neutron economy considerably, and allow much simpler designs to be considered.

(iii) Better codes, to determine the spectra in more realistic variants of the blanket. Our conclusions hinge upon the calculations made thus far, and they need checking and extension.

(iv) Vacuum pumping systems quite different from those used hitherto.

(v) The fusion-fast fission-breeder concept, particularly in the barely subcritical fission regime, to obtain a better basis of comparison with more conventional breeders.

(vi) Corrosion and related chemical problems.

(vii) Expected tritium holdup and inventory.

(viii) Expected systems operation of such reactors, from the points of view of economics, doubling time, and so forth.

(ix) Large superconducting magnetic field production.

These questions are just as important as those of plasma confinement. What is the use of plasma confinement unless we have a fair idea that the system will be feasible?

There is an interesting story of a previous search. In 1680, Christian Huygens decided that to control the force of gunpowder for peaceful purposes would be a boon to mankind, and together with his assistant Denys Papin, set out to make a controlled gunpowder engine. After some difficulties, in 1690, Papin thought of steam instead. He wrote:

> "...Since it is a property of water that a small quantity of it turned into vapor by heat has an elastic force like that of air, but upon cold supervening is again resolved into water, so that no trace of the said elastic force remains, I concluded that machines could be constructed wherein, by the help of no very intense heat, and at little cost, could produce that perfect vacuum which could by no means be obtained by gunpowder."

and invented the first steam cycle.

D. J. Rose

References

1. A. J. Impink, Jr. , Technical Report 434, Research Laboratory of Electronics, M. I. T., June 22, 1965.

2. W. G. Homeyer, Technical Report 435, Research Laboratory of Electronics, M. I. T., June 29, 1965.

3. L. N. Lontai, Technical Report 436, Research Laboratory of Electronics, M. I. T., July 6, 1965.

4. P. S. Spangler, Technical Report 437, Research Laboratory of Electronics, M. I. T., July 13, 1965.

5. L. M. Petrie, Jr., Technical Report 438, Research Laboratory of Electronics, M. I. T., July 20, 1965.

6. F. E. Dunn, "The effect of Plasma Stability on the Feasibility of a Pulsed Fusion Device," S. M. Thesis, Department of Physics, M. I. T., May 1965.

7. D. J. Rose and M. Clark, Plasmas and Controlled Fusion (The M. I. T. Press, Cambridge, Mass., 1961), Chap. 13.

8. F. L. Ribe, Los Alamos Report LA-3294-MS, 20 May 1965.

2. TURBULENT PLASMA ARC EXPERIMENT

Measurements on the macroscopic operating parameters of the hollow-cathode arc that was constructed for the study of plasma turbulence[1] have been carried out by means of Langmuir probes. The versatility of the device as a plasma source is illustrated by Fig. XVII-24, which defines the regime of continuously variable operation that can actually be attained. The plasma is highly spatially inhomogeneous, because of the anode
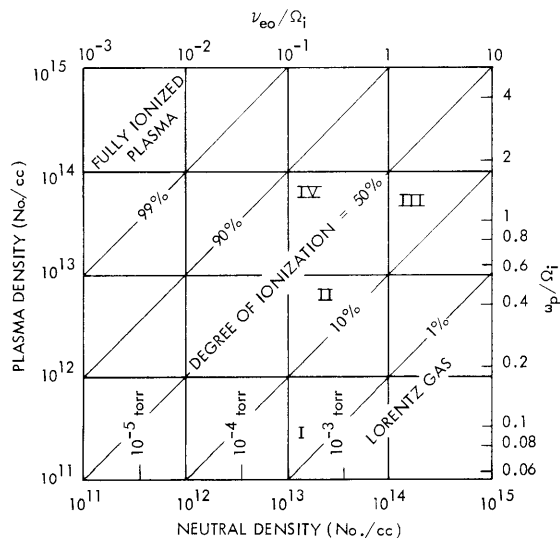

Fig. XVII-24. Regime of operation.

ν_{eo} = electron neutral collision frequency

ω_p = electron plasma frequency

Ω_i = 10^6 cps = ion cyclotron frequency characteristic of the device.

Roman numerals indicate regimes investigated by others in similar devices: I, D. Morse, R. L. E. , M. I. T; II, Alexiff and Neidigh, ORNL; III, F. Chen, Princeton; IV, S. Yoshikawa, R. L. E. , M. I. T.

baffles that also act as limiters for the primary plasma. Consequently, both the density and temperature are down by an order of magnitude in the secondary plasma as compared with those in the core. A typical radial profile taken in the midsection of the drift tube is shown in Fig. XVII-25.

The electron temperature may be varied from a few electron volts to as high as 40 ev by regulating the gas-feed rate. Because the thermalization time for electrons, ions, and species in between is in the ratio $1:(m_i/m_e)^{1/2}:(m_i/m_e)$, both the electrons and ions have Maxwellian distributions, but $T_e \gg T_i$. The parameter $n\lambda_d^3 = \left(\dfrac{\epsilon_o KT}{e^2}\right)^{3/2} \dfrac{1}{\sqrt{n}}$, which characterizes the number of particles in a Debye sphere, is approximately 100,
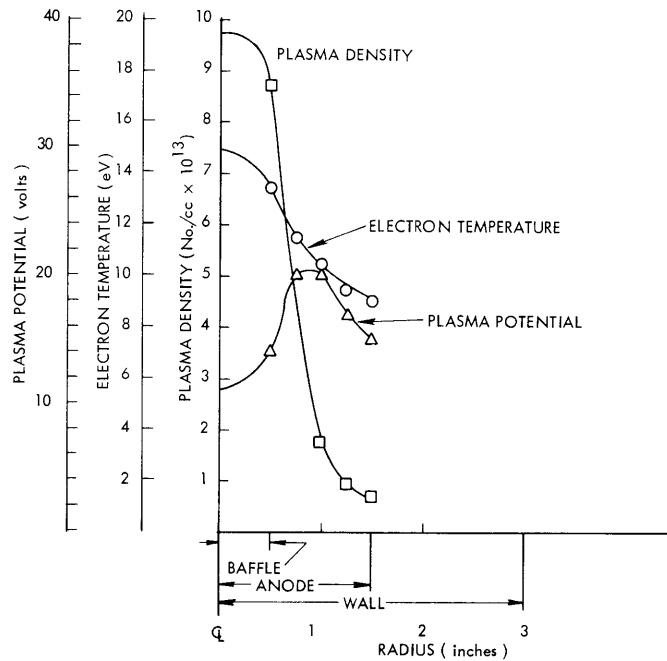
Fig. XVII-25. Radial profile.

even for $n = 10^{15}/cm^3$; therefore, the plasma may be considered in accordance with collisionless model, provided that collisions with neutrals are neglected. The condition is satisfied when the background pressure is 10^{-5} torr or lower.

Because of the presence of the magnetic field, the particle collection by the probe is impeded. Directional measurements with a plane probe have shown the expected reduction in the electron current in the direction normal to the magnetic field; however, the ion saturation current showed no significant difference even though the 1.5-mm probe dimension is comparable to the ion Larmor radius. The electron temperature and the plasma density calculated from the probe curves are independent of the orientation of the probe collection surface, which helps to lend credence to these measurements.

As is typical of arc plasmas, large-scale fluctuations have been observed in all regimes of operation; these fluctuations have been the main object of this investigation. In general, the electrostatic fluctuation spectra as measured by the floating probes are strongly dependent on the operating condition and the spatial position of the measuring probe. Figure XVII-26 is an example of the spectrum-analyzer display of the probe signals.

Present research effort has been directed toward operation in the highly ionized regime ($\gtrsim$90 per cent ionized). Further investigations have revealed the detailed structure of one dominant oscillation at a fundamental frequency of 122 kc. The oscillation propagates in the azimuthal E × B direction in the primary core of the plasma column
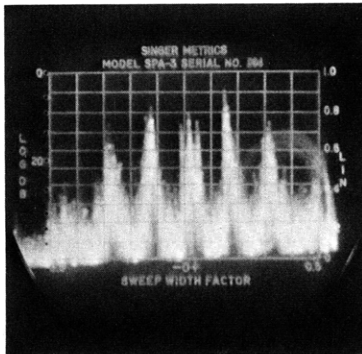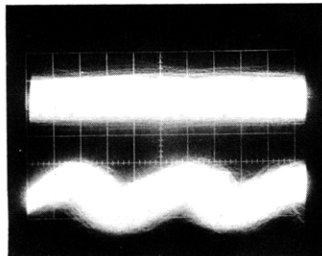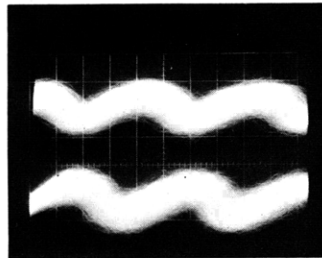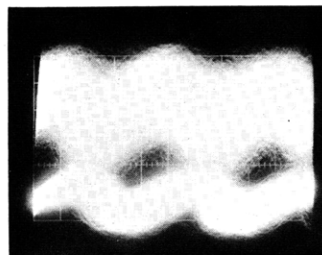
Fig. XVII-26. Spectrum-analyzer display of floating-probe signal. Sweep width, ±2 Mc; amplitude scale, 40 db full scale.

(a)

(b)

(c)

Fig. XVII-27. Correlation of probe signal displaced 90° azimuthally (sweep rate, 2 μsec/cm). Bottom trace: reference probe at floating potential. Top trace: signal as the bias on the probe is varied. (a) Bias, −80 volts to collect ion saturation current. (b) Bias, −35 volts (floating potential). (c) Bias, −10 volts.

where the radial electric field points inward and exceeds the value $E_r \gtrsim 100$ volts/meter. The oscilloscope display of two probes displaced 90° azimuthally is shown in Fig. XVII-27. Such azimuthal rotating signals have been observed by many others, and have been interpreted as an off-center rotating plasma cloud. The oscillation observed in our case differs in that it arises not from an asymmetry of the zero-order density distribution, but from a first-order fluctuation in plasma potential, as shown by the data in Fig. XVII-27.

The fundamental $m = 1$ mode is observed when there is no longitudinal electric current. If a large current flows through the plasma column, then only the $m = 2$ mode is excited. The potential amplitude of the oscillation is saturated at the level of the electron temperature. The dependence of the amplitude and direction of propagation of this mode on the radial electric field clearly suggests that this is a convective instability driven by the Hall mobility, as first discussed by Hoh[2] for a weakly ionized plasma. In the case of a highly ionized plasma, such as we have here, the instability could arise from a similar mechanism, because of the effects of the centrifugal force and viscosity, as considered by Chen.[3]

As the radial electric field vanishes or reverses direction, this organized mode changes into another low-amplitude (<1 volt) mode which propogates in the direction of the applied magnetic field with a wavelength of approximately the column length. Since $T_e \gg T_i$, an ion acoustic wave can propogate; however, this possibility is ruled out by the observed phase velocity of 3×10^4 m/sec, which is considerably greater than $V_\phi = \sqrt{\dfrac{KT_e}{m_i}} = 5 \times 10^3$ m/sec for ion acoustic waves. The exact nature of this observed electrostatic wave is not clear, at present. The possibility that this is a universal drift wave driven by the pressure gradient and stabilized by the finite ion Larmor radius has not yet been investigated.

Because of the existence of growing mode(s) in the core, where the amplitude of the potential fluctuation is saturated, wave-wave interaction must be important in this region, and one expects to observe a fully developed turbulent spectrum with the growing modes superimposed on it as the source for these turbulent plasma "eddies". Outside the core, where the mechanism for growth is absent, or is very slow, only the fundamental modes can be observed on a quiescent background. That this is a reasonable model is borne out by the spectrum-analyzer data taken with probes at varying radial position, as shown in Fig. XVII-28. Near the center of the plasma column (Fig. XVII-28a), two dominant fundamental modes—a high-frequency oscillation at 122 kc discussed above, and a low-frequency mode at 30 kc which has not yet been properly identified — are superimposed on a turbulent background of Kolmogoroff-type spectrum obeying an estimated power law of $\omega^{-1.5}$. The significance of this value as compared with the $K^{-5/3}$ power law for hydrodynamic turbulence is still not understood, since

the nature of plasma turbulence is significantly different from that of ordinary hydro-dynamic turbulence. Note the cutoff of the spectrum at 300 kc which is the ion cyclotron frequency for the applied field of 1.3 kgauss. This cutoff is expected, because of the resonant heating of the plasma ions.
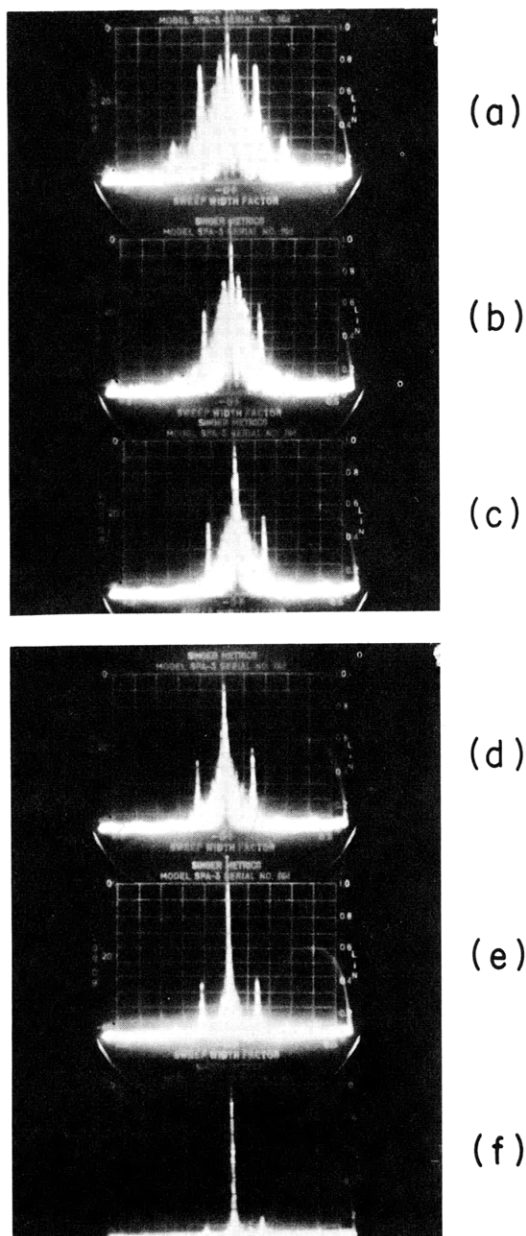
Thus the life history of a fluctuation in the core can be described in three stages: (i) a random fluctuation grows exponentially, because of the instability mechanism described by the linear theory; (ii) growth rate is checked when the fluctuating plasma potential is so large that particles can no longer feed the oscillating energy, and nonlinear wave-wave interaction causes the oscillations to diffuse in frequency and break up into small scale "eddies"; (iii) the energy in the waves is finally dissipated, thereby heating the plasma ions by cyclotron resonance inter-actions.

As the probe is gradually withdrawn from the center of the plasma column, the background spectrum gradually dis-appears (Fig. XVII-28b-e) until finally only the single excited wave is observed (Fig. XVII-28f).

The model is further supported by the radial profile shown in Fig. XVII-25. The plasma core is defined by the baffle, whose diameter is 1 inch. Therefore, for $r < 0.5$ in., the den-sity profile is relatively flat, because of the violent turbulent mixing. As a consequence, a sharp density gra-dient is set up across the secon-dary plasma where particles escape by weaker turbulence, or perhaps

(a)

(b)

(c)

(d)

(e)

(f)

Fig. XVII-28. Radial dependence of the turbulent spectrum (sweep width, ±0.5 Mc). Radial position from center of column: (a) 0.25 in.; (b) 0.5 in.; (c) 0.75 in.; (d) 1.0 in.; (e) 1.25 in.; (f) 1.5 in.

even by classical diffusion.

Our investigation will continue for the purposes of identifying other existing modes of oscillation, obtaining time-resolved measurements of the fluctuating parameters, applying mixing-length analysis to the turbulent core, and studying the mechanism for the transport of the plasma particles in the turbulent state.

J. C. Woo

References

1. J. Woo, Quarterly Progress Report No. 76, Research Laboratory of Electronics, M. I. T. , January 15, 1965, pp. 130-133.

2. F. Hoh, Phys. Fluids $\underline{6}$, 1184 (1963).

3. F. Chen, Report MATT-214, Princeton University, September 1963.

C. Plasma and Magnetohydrodynamic Flows, Waves, and Instabilities*

Academic and Research Staff

Prof. W. D. Jackson
Prof. E. S. Pierson

Graduate Students

K. R. Edwards
K. T. Gustafson

P. H. B. Kloumann
C. A. McNary

RESEARCH OBJECTIVES

Our research deals with MHD flow and wave phenomena, particularly those of engineering interest in which a low or moderate magnetic Reynolds number is involved. Both plasmas and liquid metals are employed in the experimental aspects of our work, and the development of measuring techniques receives particular attention.

During the coming year, we shall extend our work in Velikhov instabilities to slightly ionized plasmas to include additional effects such as nonequilibrium ionization. Theoretical and experimental studies of induction-driven flows will continue with emphasis on the entry problem and the interactions of traveling fields with free jets.

W. D. Jackson

XVII. PLASMAS AND CONTROLLED NUCLEAR FUSION

D. Magnetohydrodynamic Flows and Shock Waves[*]

Academic and Research Staff

Prof. A. H. Shapiro
Prof. W. H. Heiser

Graduate Students

F. W. Fraim
R. N. Harvey
M. H. Waller

RESEARCH OBJECTIVES

The primary goal of our research is the improvement of the capability of the magnetically driven shock tube for producing shock-heated test gas. At present, the measured quantity of test gas is less than can reasonably be expected, and explanations for this behavior are being sought. For example, a series of experiments is now being performed which is intended to reveal the magnitude of the Hall currents that accompany the driving current. The presence of excessive Hall currents will indicate that the effective conductivity is too low for efficient shock-tube operation. A series of experiments is also planned in which the heat transfer to the wall will be measured by means of a radiation wall heat-transfer probe. The presence of excessive wall heating will indicate that the magnetic field fails to prevent diffusion to the walls.

A new aspect of our research is an interest in magnetohydrodynamic flows. At present, we are carrying out two fundamental experiments. In the first, we are measuring the influence of an axial magnetic field upon fully developed turbulent pipe flow. The planned experiments will provide exceptionally large magnetic interaction parameters.and incorporate a hot-wire probe in order to detect turbulence. In the second, we shall measure the influence of a magnetic field transverse to a cylinder upon the location of the point of separation and the magnitude of the drag force in laminar flow.

W. H. Heiser